Some Overlooked Antenna Basics for DX and Off-World Communications

L. B. Cebik, W4RNL
1434 High Mesa Drive
Knoxville, TN 37938-4443
e-mail: cebik@cebik.com

VHF and UHF operators have the opportunity to communicate in ways denied the HF operator. We can use satellites and even the moon as off-world aids (or challenges) to communication. We can use tropospheric ducting and other even rarer atmospheric phenomena to lengthen the communications path. In the process of mastering these operating skills, we soon discover that transceivers are--for all their complex circuitry and operating features--the simplest and most constant part of our work. The crucial variable is the antenna.

There are two questions that we might pose to antennas. 1. How do I build (or, heaven forbid, buy) one? That question I shall bypass today. 2. What do antennas do once I build one (or more)? That question is my topic.

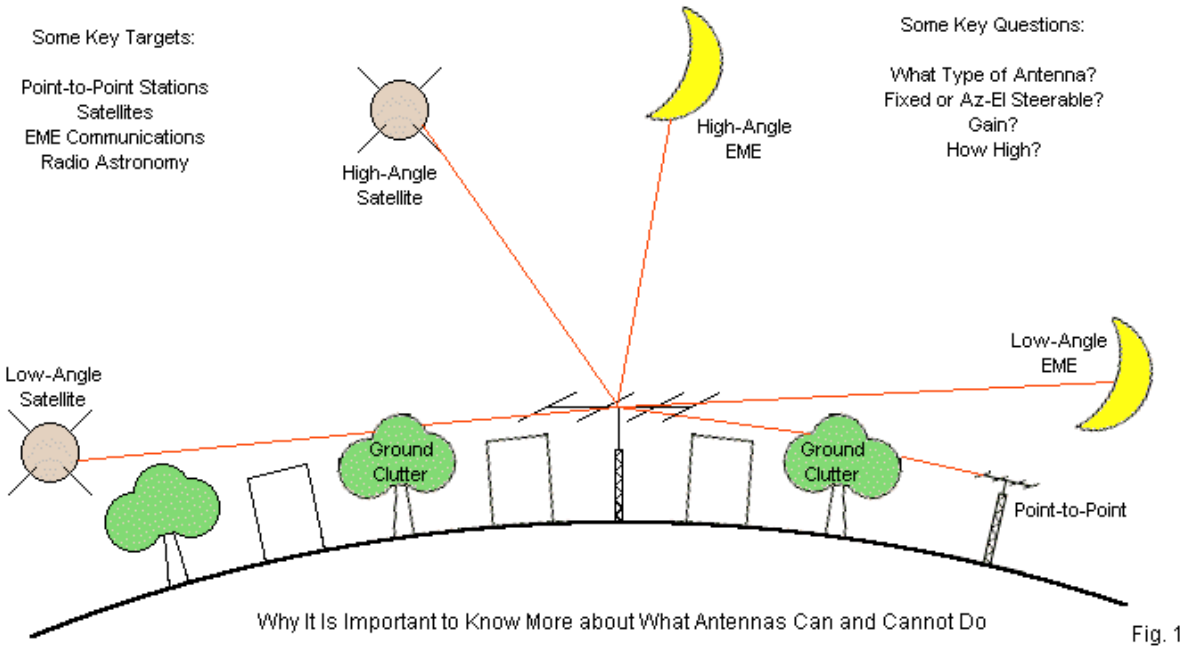

Fig. 1

Fig. 1 illustrates some of the complexities facing the VHF and UHF operator who wishes to do everything (except use local repeaters, a topic for another day). Initially, the operator imagines a simple fixed omni-directional antenna. But capturing the distant point-to-point station and the rapidly moving satellite in the presence of ground clutter raises questions. It seems that even to receive weather maps around 137 MHz requires an antenna that is high enough to see over the trees and buildings to catch the satellite while it is at a low elevation angle. Similar considerations apply to the distant station, within the gain limits of an omni-directional antenna. I would not disturb this blissful formula for success if it always worked. As we shall see, it does not always work, and for reasons related to basic antenna performance in the presence of the very thing that supports all of that clutter--the ground.

The more advanced operator resorts to big antennas on high towers with rotational control for both azimuth and elevation. He or she tends to imagine that the long Yagi, quad, or axial-mode helix puts forth a teardrop radiation pattern both vertically and horizontally so that all he or she needs to do is to aim the antenna at the target. Regardless of whether the satellite or the moon is low or high in the sky, gain and aiming skill are the only two considerations of note. (I shall assume that all operators are courteous and

reduce power to the minimum needed for satellite communications, saving the large amplifier for EME, point-to-point, and coffee-warming efforts.) Unfortunately, there is more to the aimable antenna story than mere aiming.

Finally, there is the matter of polarization. Just when amateurs had gotten used to distinguishing between vertical and horizontal polarization, antenna engineers determined that circular polarization is superior--as long as we match the left-hand or the right-hand version used at the other end of the communications path. The idea of circular polarization became commonplace as soon as folks realized that a moving satellite target with linear elements would change polarization as it moved across the sky. But circles never change. Amateurs have rarely paused to realize that circular and linear polarizations are simply special cases of elliptical polarization. They have also rarely looked into the relationship between the vertical and horizontal components of a total far field to see how they might be related to the left- and right-hand components of the same field viewed circularly or elliptically. These fundamental ideas are important to understanding just how good or poor various antenna designs may be as generators of circularly polarized radiation--and receivers of the same.

These notes will try to organize some of these basic but overlooked ideas into a semblance of a coherent whole. We shall move from fixed antennas to aimable antenna and, finally, to circularly polarized antennas. One step will provide a partial foundation for the next. Because we do not have unlimited space or time, we shall sample common (and a few uncommon) antennas to illustrate the ideas. In the process, we may even clear away a few persistent myths that have been generated by learning our antenna ideas in limited sound bites, small pictures, and excessively simple equations. There are more things in the world of antennas than are dreamt of in your philosophy, Horatio.

Fixed Omni-Directional Antennas

When amateurs first start to dream of satellite communications or of receiving weather information from satellites, they tend to think simple and inexpensive thoughts. They want to install a basic omni-directional antenna with enough gain to allow error-free reception from and a solid connection to a communications satellite. Since satellites may appear almost anywhere in the hemisphere surrounding a given location, an ideal pattern emerges, as portrayed in **Fig. 2**. The small square on the Z-axis is an arbitrary antenna, since the pattern is not achievable.

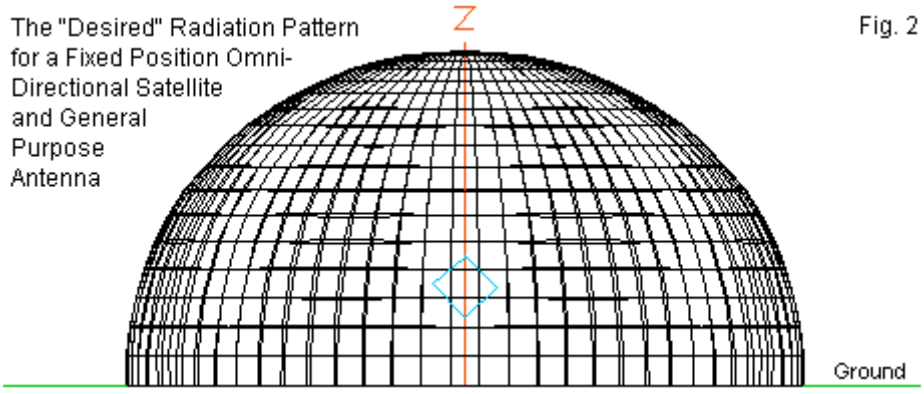

Fig. 2

There are two problems that prevent us from obtaining the ideal omni-directional pattern. One difficulty is ground clutter (see **Fig. 1**). It absorbs, reflects, or refracts very low angle signals. That fact prompts us to raise the antenna to "see over" the clutter in order to reach the horizon. Height improvement works to some extent for point-to-point communications, although intervening clutter may still provide interfering reflections unless we place the antenna very high indeed. However, for satellite work, the technique is not only relatively futile, it can be self-defeating. Satellites are in the extreme far field of any antenna, and the very existence of the ground at any distance will prevent us from creating an ideal omni-directional pattern.

We might here go back to the textbooks and supply an array of equations by which to prove our point. However, it may be more instructive simply to model some of the most widely used omni-directional antennas and sample their patterns at various heights above ground. Each sample will use 1.5-mm diameter aluminum elements at 300 MHz (more precisely, 299.7925 MHz, where 1 meter = 1 λ). Each 2-element antenna will use a 90° phase-difference between elements to achieve the omni-directional pattern. There are numerous techniques to achieve turnstiling--or what engineers prefer to call quadrature feed--but most amateurs will likely use a ¼-λ electrical section of transmission line with the same impedance as the individual elements in the antenna. The net feedpoint impedance will be ½ the impedance of the individual element. When we place the antenna above ground, we shall use average soil (conductivity 0.005 S/m, relative permittivity 13). In this initial part of our work, we shall only be interested in the total far field of the antenna. We shall save the vertical, horizontal, and circular components for the last part of our work.

1. *Turnstiled Dipoles*: Perhaps the oldest quadrature-fed antenna is a pair of turnstiled dipoles. A version of this antenna has appeared in every *ARRL Antenna Book* since satellites first appeared, and the antenna predates that event by decades as an upper HF and lower VHF omni-directional antenna. The antenna found wide use in the days before repeaters, when virtually all VHF communications in the amateur bands used horizontally polarized antennas.

The upper portion of **Fig. 3** shows the outline of the dipole turnstile. The appearance gave us the antenna name and that name eventually transferred to the simple feed method. Be certain that the feed system is properly matched at every step, because the SWR curve will remain impressively low long after the free-space patterns to the upper right have gone to pot. The beamwidth of a dipole prevents a perfect E-plane circle, but the squared circle varies only by about 1 dB from maximum to minimum. The H-plane pattern shows that the simple turnstile radiates more strongly broadside to the antenna than off the edges, an important reason why folks tried other designs.

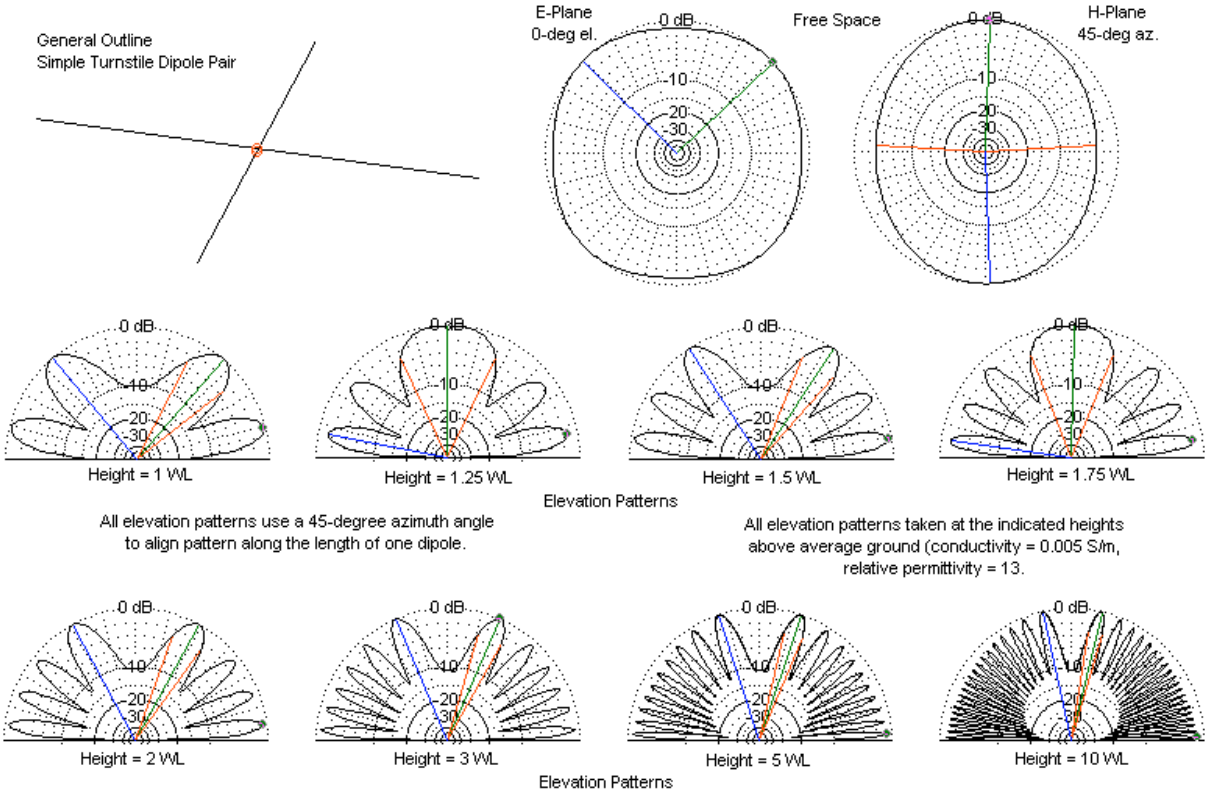

Sample Total-Field Patterns of a Turnstile Dipole Pair

Fig. 3

The lower part of **Fig. 3** contains the critical information about the elevation patterns of a simple dipole turnstile as we gradually raise the height of the wires above average ground. **Table 1** summarizes the data.

Table 1. Critical Performance Data for a Dipole Turnstile at Various Heights above Average Ground

Height (λ)	Gain (dBi)	Elevation Angle Of Peak Gain	Lowest Elevation Angle (degrees)	Gain at Lowest Elevation Angle (dBi)
1	4.85	49	14	4.61
1.25	5.98	90	11	4.63
1.5	5.15	57	9	4.73
1.75	5.99	90	8	4.76
2	5.32	61	7	4.83
3	5.52	67	5	4.89
5	5.71	72	3	5.00
10	5.85	77	1.5	5.06

The elevation pattern of the dipole turnstile has deep nulls between elevation lobes at any height above ground. Even at a height of 10 λ, the null regions where a signal may drop more than 3-dB relative to the lobe value is larger than the region where the signal is less than 3-dB below peak lobe value. Note also that the zenith region (directly overhead) changes as a function of the antenna height, with a deep null at integral height multiples of ½ λ and a lobe at odd multiples of ¼ λ. In general, the basic dipole turnstile is quite unsatisfactory for general satellite communications and for weather satellite reception, even though it might be useful for local horizontal point-to-point communications.

2. *Turnstiled Dipoles with a Planar Reflector Screen*: The immediate amateur development to improve the dipole turnstile was to add a screen below the antenna. The impression that this maneuver leaves is that obtaining more gain cures everything. A proper planar reflector extends at least 0.5-λ beyond the limits of the driven antenna elements in every direction. In this case, we may arrange the element to point toward the corners of a square screen in order to minimize excess screen size. Nevertheless, an adequate planar reflector will be about 1.4 λ per side, as shown at the top left of **Fig. 4**. The free-space patterns should suffice to forewarn us that this antenna system will have very limited utility. The antenna shows good gain and an excellent free-space front-to-back ratio. But as the data in **Table 2** reveal, along with the patterns in the lower half of **Fig. 4**, the antenna is good only for satellites directly above us and is worse than the simple turnstile dipole system near the horizon.

Table 2. Critical Performance Data for a Dipole Turnstile with a Planar Reflector at Various Heights above Average Ground

Height (λ)	Gain (dBi)	Elevation Angle Of Peak Gain	Beamwidth (degrees)	Lowest Elevation Angle (degrees)	Gain at Lowest Elevation Angle (dBi)
1	8.75	90	64	13	-0.33
1.25	8.00	90	77	11	-0.47
1.5	8.63	90	74	9	-0.53
1.75	7.98	90	74	8	-0.60
2	8.62	90	74	7	-0.59
3	8.68	90	68	5	-0.68
5	8.78	90	71	3	-0.53
10	8.88	81	65	1.5	-0.50

The table lists the half-power beamwidth of the antenna patterns at each height, as a measure of how much of the 180° hemisphere might be missing from coverage. The patterns in **Fig. 4** also show several other interesting facets of pattern development with increasing height. For example, note the pattern for a height of 10 λ above ground. It shows 2 peaks that represent what amounts to a circle of maximum gain with a null at the exact zenith angle. As well, the low angle lobes and nulls, although smaller than those for the simple dipole turnstile, remain in place, since they are a result of the antenna's height and not of its specific design.

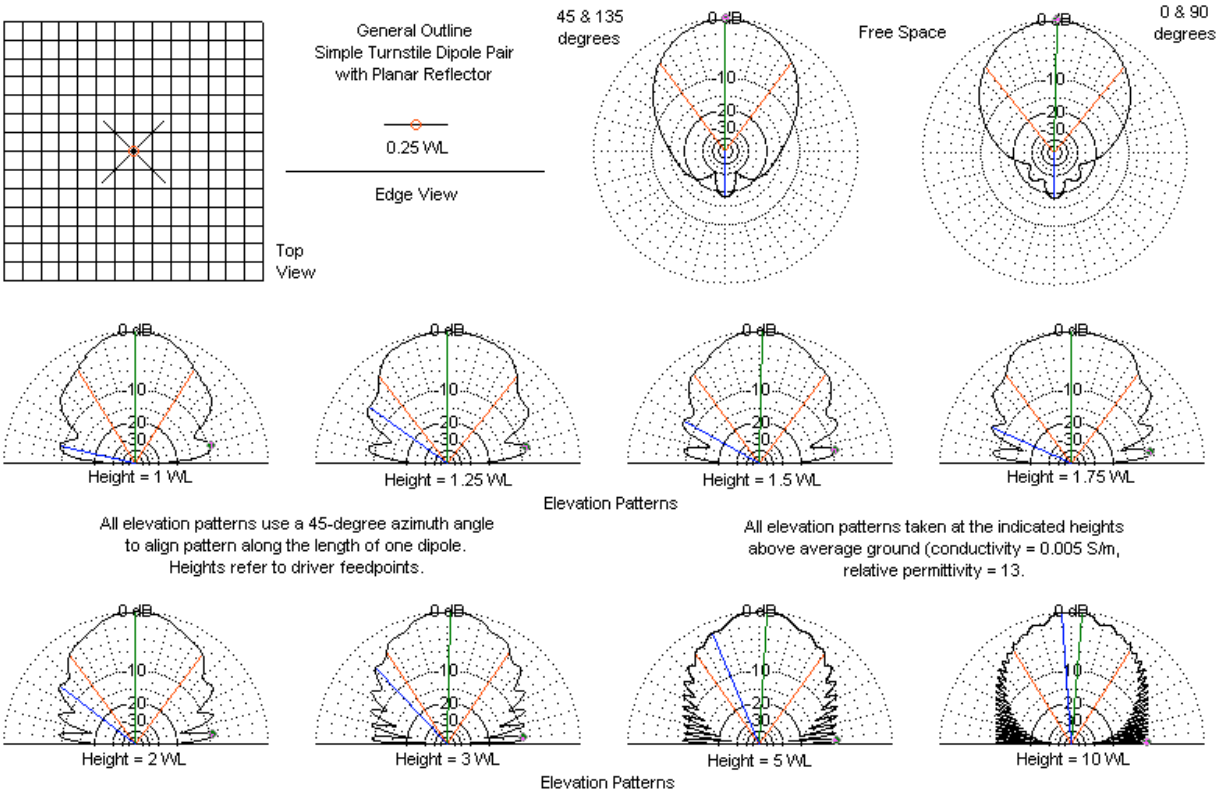

Sample Total-Field Patterns of a Turnstile Dipole Pair with a Planar (Screen) Reflector

Fig. 4

The third aspect of pattern development with increasing height for antennas that point generally upward is the development of high-angle ripples in the main forward lobe. These ripples tend to be most prominent in antennas that use crossed elements to achieve circular polarization. However, we shall encounter them to one degree or another in the patterns of all antenna raised to the vertical.

In the end, the dipole turnstile with an adequate planar reflector does not serve well as a fixed position omni-directional antenna for any service. However, in the upper UHF region (70 cm and upward), it may serve as a simple and effective aimable antenna, if 8 to 8.5 dBi is adequate gain for the operation. Do not skimp on the screen size, because gain will drop quite rapidly as we downsize the reflector dimensions.

3. *Turnstiled Quad Loops*: We can generally create a turnstile pair out of any element that has a linear dimension and makes no more than a flat plane. The quad loop is a variation on the dipole. In fact, it is roughly 2 dipoles spaced ¼ λ vertically, each bent so that the ends just touch. If we set two quad loops at right angles so that the feedpoints are close but do not touch, we can add a ¼-λ phasing line between them, but we must adjust the characteristic impedance of the line to match the individual self-resonant impedance of the loop--about 125-130 Ω. The feedpoint impedance of the turnstiled quad will be half that value. It appears not to matter if the top crossing points do or do not touch.

Turnstiled quads came into play as omni-directional antennas with slightly more gain than the dipole turnstile. They come in two varieties, depending on whether we start with square quad loops or with diamond quad loops. **Fig. 5** shows the general outline of both versions, along with free-space patterns. Notice that in each case, the patterns form a nearly perfect sphere, rather than showing the egg-shape of the dipole turnstile. Hence, we expect a small increase of gain in the E-plane. The square loop version unfortunately arose in a decade in which cute names were more important to antennas than performance. Hence, someone dubbed the antenna the "eggbeater," a name best forgotten, lest someone rename the turnstiled diamond loops the "whisk."

Fig. 5

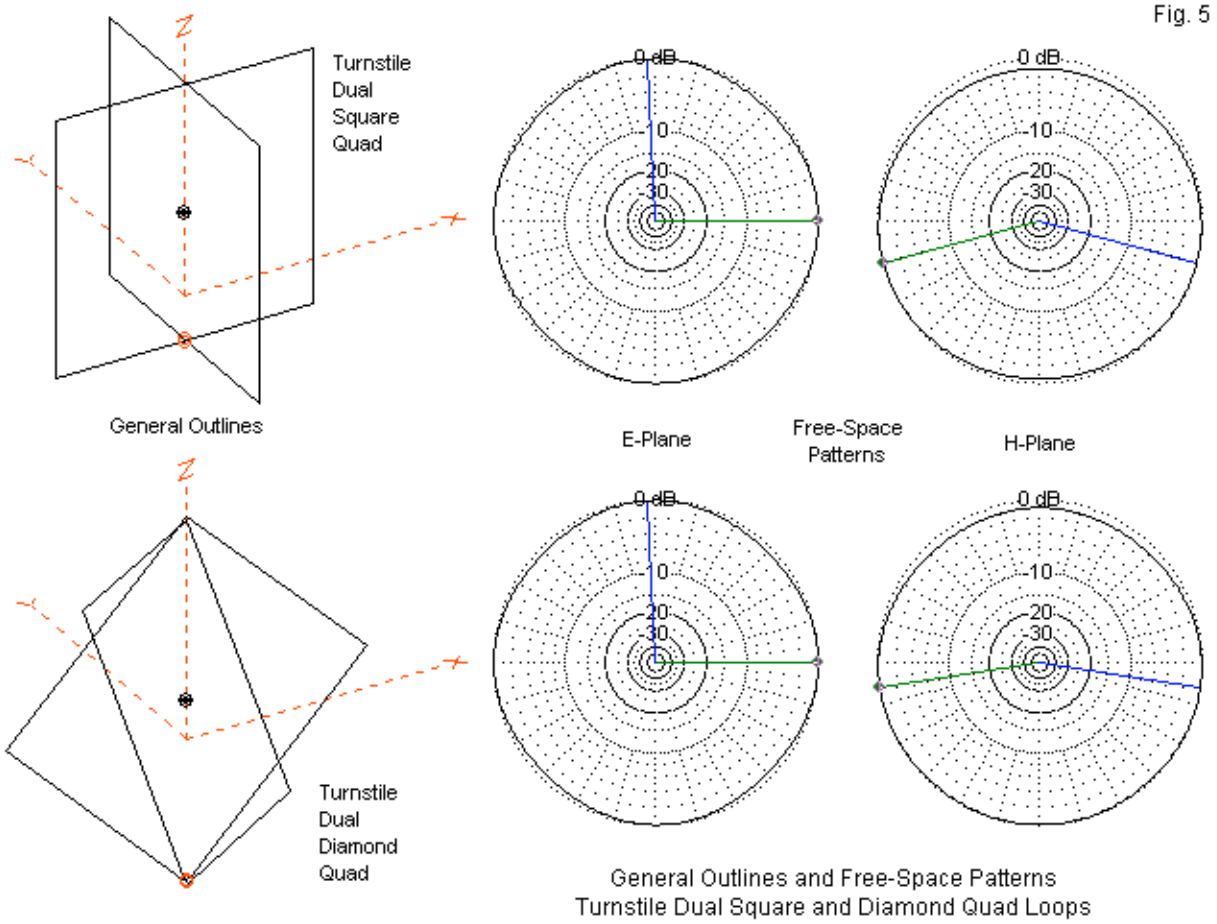

General Outlines and Free-Space Patterns
Turnstile Dual Square and Diamond Quad Loops

As **Table 3** shows, there is very little performance difference between the two versions of the same antenna. Since the heights of the antennas depend on the bottom-most point or the feedpoint, the slightly taller diamond loop antenna shows values that reflect the small increase in average height. See **Fig. 6** for the patterns of the square quad loops over ground and **Fig. 7** for the corresponding diamond loop quad patterns. Note that in both cases, the maximum gain applies to the lowest elevation lobe in the pattern. The maximum gain in this lobe is about 1 dB greater than for a dipole turnstile at the same feedpoint height. As the catalog of patterns shows, the gain improvement is not as significant as it might initially seem. In general, we choose between the 2 versions of the turnstiled quads most often due to a preference for certain construction methods. The models used here at 300 MHz use 1.5-mm diameter elements, but common wire sizes will do as well.

Table 3. Critical Performance Data for Turnstile Quad Loops at Various Heights above Average Ground

A. Square Quad Loops			B. Diamond quad Loops	
Height (λ)	Gain (dBi)	Elevation Angle Of Peak Gain	Gain (dBi)	Elevation Angle Of Peak Gain
1	5.86	12	5.92	12
1.25	5.70	10	5.84	10
1.5	6.01	9	6.08	8
1.75	5.86	7	6.00	7
2	6.09	7	6.14	6
3	6.10	4	6.17	5
5	6.29	3	6.35	3
10	6.34	1.5	6.41	1.5

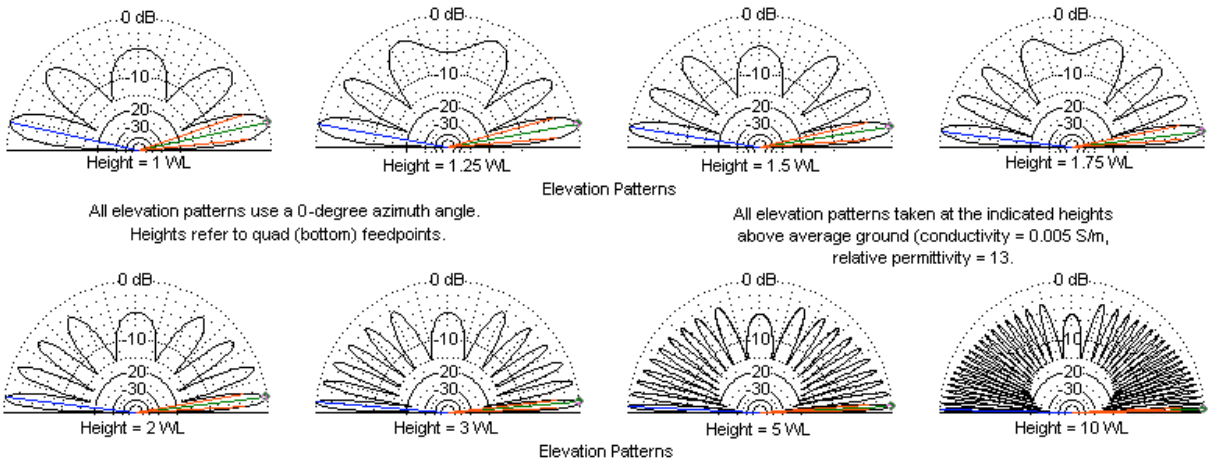

Sample Total-Field Patterns of a Turnstiled Square Quad Pair

Fig. 6

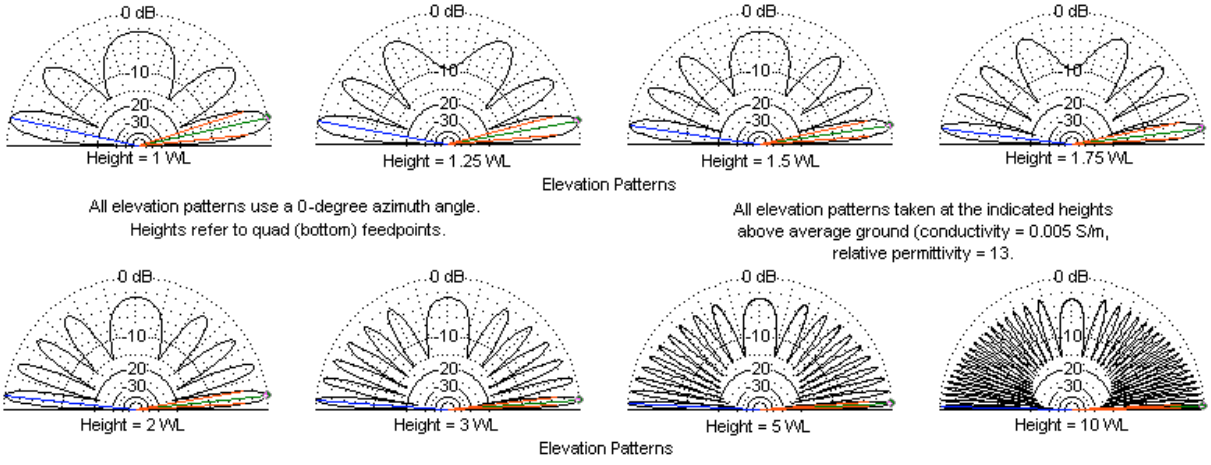

Sample Total-Field Patterns of a Turnstiled Diamond Quad Pair

Fig. 7

Unlike the dipole turnstile, the zenith-angle domes occur at integral multiples of a half-wavelength, with upward nulls occurring at odd multiples of ¼ λ. Otherwise, we have no reason to consider the turnstiled quad loops further as candidates for fixed satellite communications service. They display all of the nulls shown by the dipole turnstile for all practical heights. Therefore, they suffer from the same variability of signal strength as a satellite moves across the sky.

4. *Turnstiled Moxon Rectangles*: The number of lobes and nulls in any turnstile horizontal antenna is a function of the height of the antenna above ground. Hence, we cannot eliminate them. However, we can go some distance in reducing the null depth by selecting the right kind of antenna to fit into the turnstile. One key factor is the inherent H-plane beamwidth of the antenna element in isolation. The Moxon rectangle is a 2-element parasitic beam with the element ends folded back toward each other. It has a very broad beamwidth in the H-plane, and has enough side radiation off the element tails to partially fill the nulls at low angles. The resulting pattern is far from perfect, but it goes a considerable distance in the right direction.

Fig. 8 shows the outline of a turnstiled pair of Moxon rectangles at the upper left. Although the driver centers require enough separation for the phase line, the reflector elements may touch at their centers. We can design the rectangle for a 50-Ω feedpoint. The phase line will require a 50-Ω section of coax, but the 25-Ω net feedpoint impedance will require transformation back to 50 Ω. Alternatively, we may design

the rectangle for a 95-Ω feedpoint and use coax of that value for the phase line. The resulting net feedpoint impedance is close enough to 50 Ω not to require any special matching.

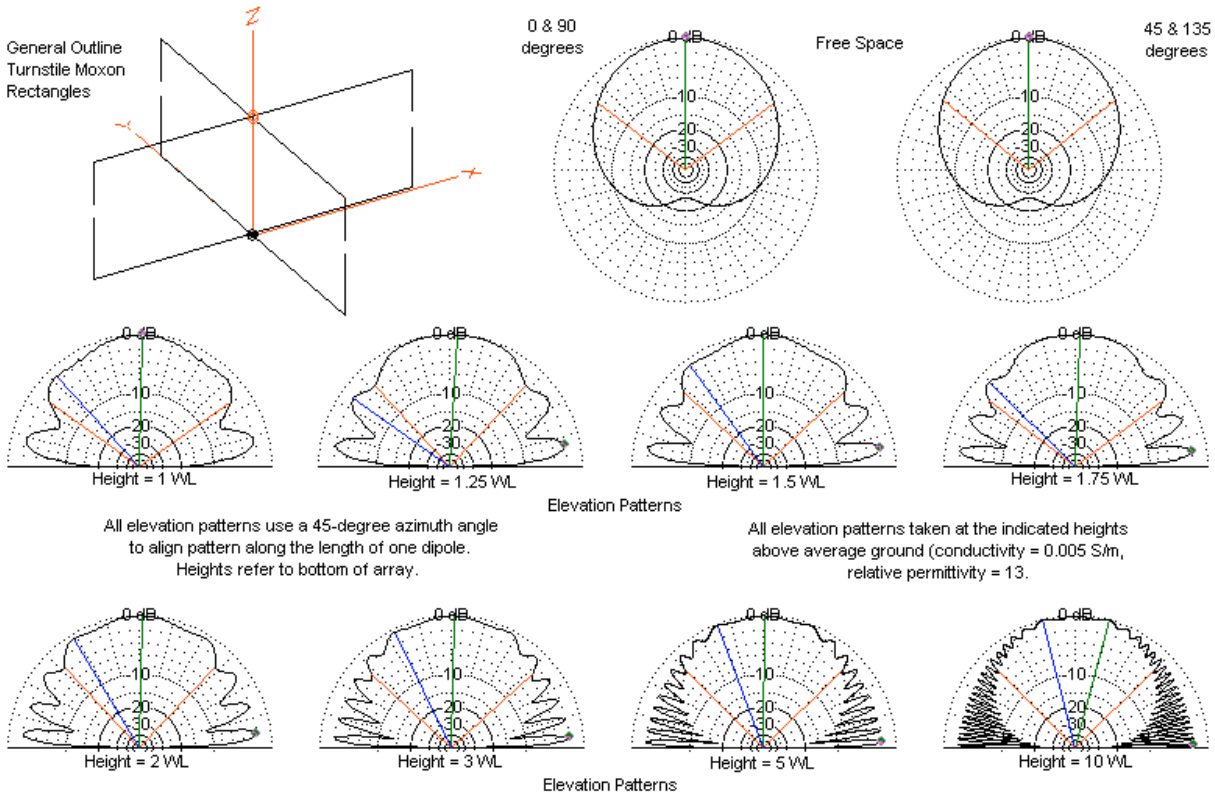

Sample Total-Field Patterns of a Turnstile Moxon Rectangle Pair

Fig. 8

The free-space patterns show the wide beamwidth that results in the more modest nulls in the patterns taken above ground. As revealed in **Table 4**, the beamwidth of the upper dome is always at least 90°.

Table 4. Critical Performance Data for Turnstiled Moxon Rectangles at Various Heights above Average Ground

Height (λ)	Gain (dBi)	Elevation Angle Of Peak Gain	Beamwidth (degrees)	Lowest Elevation Angle (degrees)	Gain at Lowest Elevation Angle (dBi)
1	5.82	90	109	13	3.70
1.25	5.87	90	86	11	3.70
1.5	5.82	90	94	9	3.78
1.75	5.88	90	105	8	3.77
2	5.82	90	87	7	3.83
3	5.82	90	95	5	3.84
5	5.82	90	91	3	3.98
10	5.87	90	91	1.5	4.04

The turnstiled Moxon rectangles achieve much superior evenness of performance at higher elevation angles than any of the fixed antenna candidates that we have so far surveyed. The maximum gain is remarkably consistent regardless of the height of the antenna above ground, largely due to the fact that the antenna has its own highly effective reflector. Direct downward radiation is almost non-existent.

However, as shown by the elevation plots in **Fig. 8**, the antenna only goes part way toward smooth performance at lower elevation angles. The antenna configuration limits, but does not eliminate the nulls between elevation lobes. As we increase the height of the antenna above ground, we encounter the same growth in the numbers of lobes and nulls that we have seen in all of the fixed satellite antenna candidates. If we cannot satisfy our operating needs at angles higher then about 30° above the horizon, then we must continue the search for a better fixed-position antenna.

5. *The Modified Lindenblad*: In 1941, N. E. Lindenblad developed and patented a design for a circularly polarized antenna to use at the television station atop the Empire State Building. The necessities of World War II delayed the actual construction of a Lindenblad antenna into after the war, and then, the builders intended it for possible aviation use. (See N. E. Lindenblad, " Antennas and Transmission Lines at the Empire State Television Station," *Communications*, vol. 21, April, 1941, pp. 10-14 and 24-26, and G. H. Brown and O. M. Woodward, "Circularly Polarized Omnidirectional Antenna," *RCA Review*, vol. 8, June, 1947, pp. 259-269.) The Lindenblad has undergone re-invention and modification in recent times without due credit to the original developers. The references should rectify this situation. See **Appendix 1** for a comparison of the original Lindenblad with the modified version shown here.

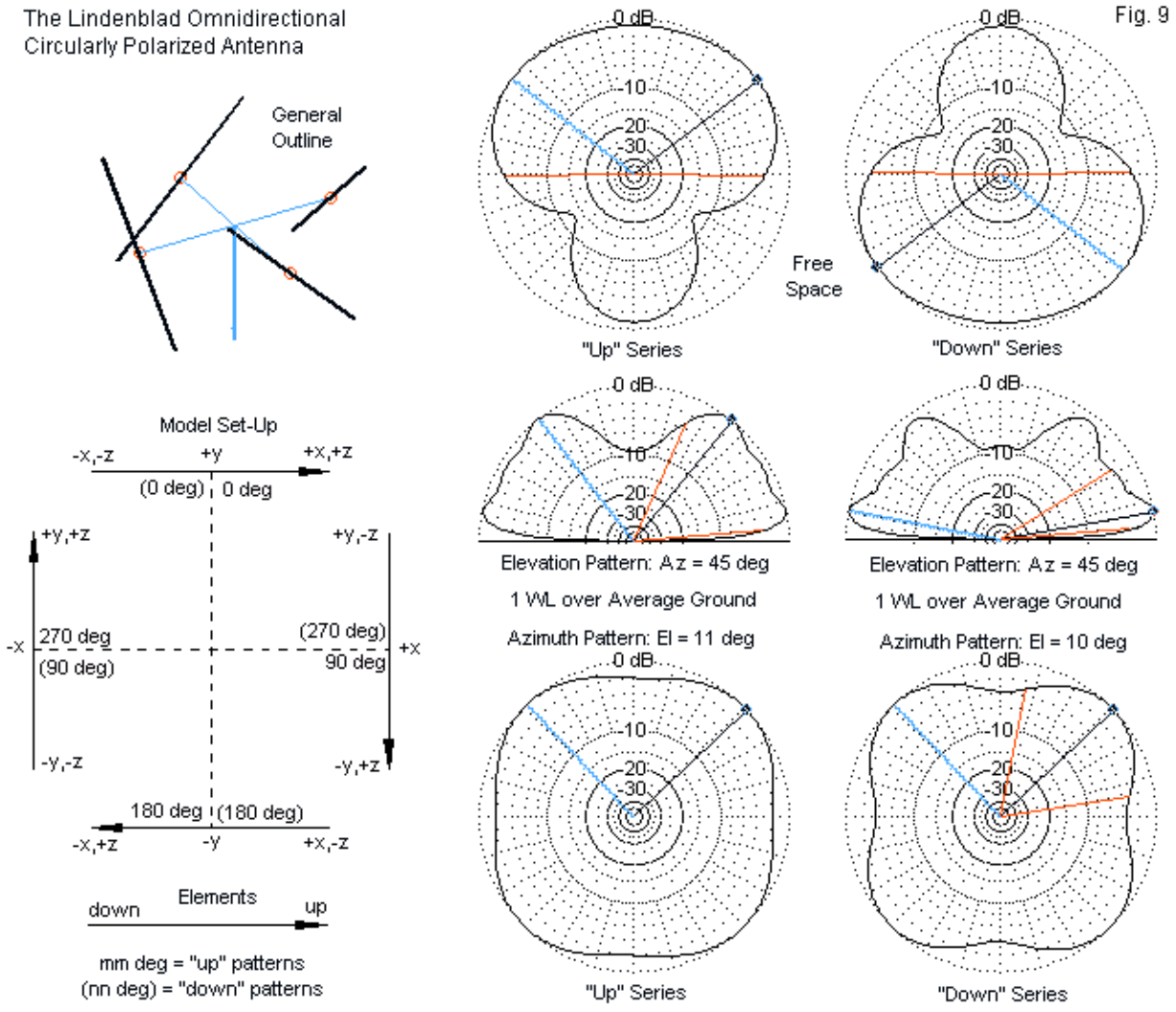

Fig. 9 shows the outline of the modified Lindenblad on the left, along with instructions on how to model it. It consists of 4 dipoles forming a square. However, each dipole is slanted 45°. Since one may

easily mess up the model, the orientations of the elements and the sequence of current source phasing appear in the diagram. Note that we select one element as the prime element and progressively increase the phase angle of each succeeding source by 90° in a clockwise direction to obtain the desired "up" series. (The original Lindenblad fed each dipole in phase to achieve low-angle circular polarization. However, as the Appendix will show, the resulting antenna has severe limitations for satellite use. Hence, the use of progressive quadrature feed has advantages in satellite service.) If we leave the elements oriented as before but use a counterclockwise progression of phase angle increases, we obtain the less-desired "down" series. (Reversing both the element orientations and the progression of phase angles will result in an "up" series.)

The right side of **Fig. 9** shows the differences between the up and down series. (The original Lindenblad has a free-space pattern that is symmetrical with respect to the array centerline.) The differences are vivid in the free-space pattern, but less so in the patterns above ground by 1 λ. However, the gain is smoother as we increase the elevation angle in the up series, and the differences between maximum and minimum gain in the azimuth pattern are smaller. The modified Lindenblad was not designed to create a high angle dome, but to provide omni-directional television transmission suitable for reception by both horizontal and vertical antennas in the early days of urban TV. Hence, the upward null was not considered a hindrance to good performance.

The optimal spacing for the dipoles in a modified Lindenblad array has come in for some discussion. The upper portion of **Fig. 10** provides some guidance. The spacing values reflect a center point, so the actual spacing between facing dipoles is twice the listed value. A spacing of 0.5 λ provides perhaps the best obtainable pattern over average soil for elevation angles up to about 50°. 0.6-λ spacing might extend the elevation angles 10° further upward, but with somewhat higher ripple in the signal strength.

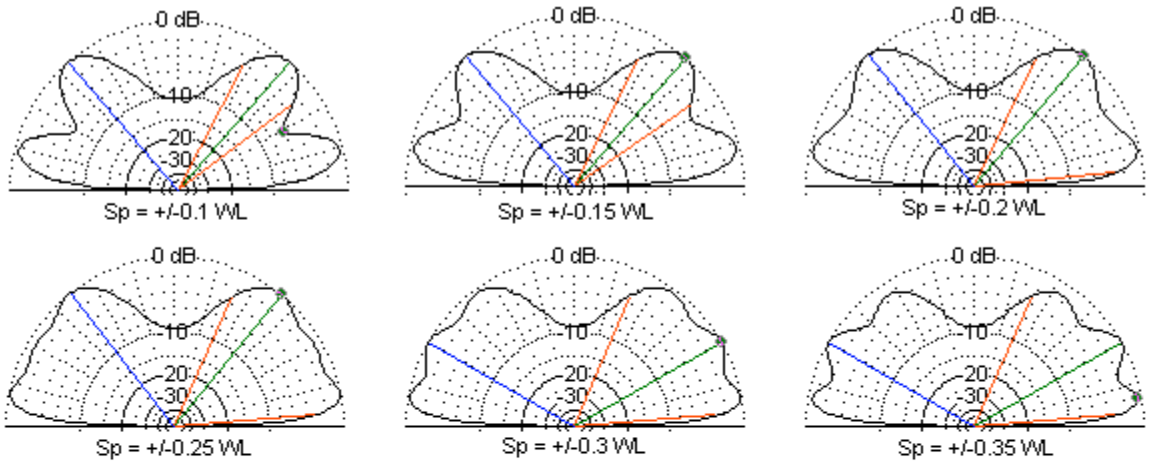

Lindenblad Elevation Patterns at 1 WL above Average Ground
Using Variable Spacing Between Facing Dipoles

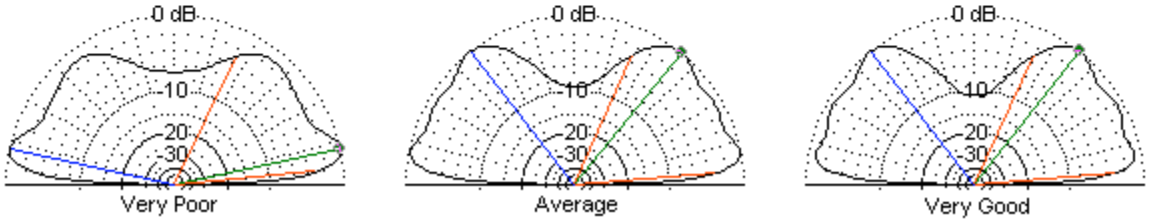

Lindenblad Elevation Patterns at 1 WL above Various Ground Qualities
Using +/-0.25-WL Spacing Between Facing Dipoles

Fig. 10

The lower part of **Fig. 10** provides data for the effects of soil quality on the pattern shape, using a spacing of 0.5 λ between facing dipoles with the feedpoints 1 λ above ground. Very poor soil shows some pattern degradation, but the patterns for average and better soil are remarkably consistent.

Table 5 provides data on the modified Lindenblad array set at various heights above average ground. See **Fig. 11** to correlate the data with elevation patterns. In general, the Lindenblad is subject to the same variations in zenith-region radiation as the single turnstile dipole. However, the antenna excels in evenness of performance at lower elevation angles.

Table 5. Critical Performance Data for a Lindenblad Array
at Various Heights above Average Ground

Height (λ)	Gain (dBi)	Elevation Angle Of Peak Gain	Beamwidth (degrees)	Lowest Elevation Angle (degrees)	Gain at Lowest Elevation Angle (dBi)
1	3.36	51	62	11	3.25
1.25	4.98	90	52	10	3.56
1.5	4.02	8	65	8	4.02
1.75	5.01	90	44	7	4.27
2	4.55	6	9	6	4.55
3	5.19	4	5	4	5.19
5	5.92	3	3	3	5.92
10	6.51	1.5	1.5	1.5	6.51

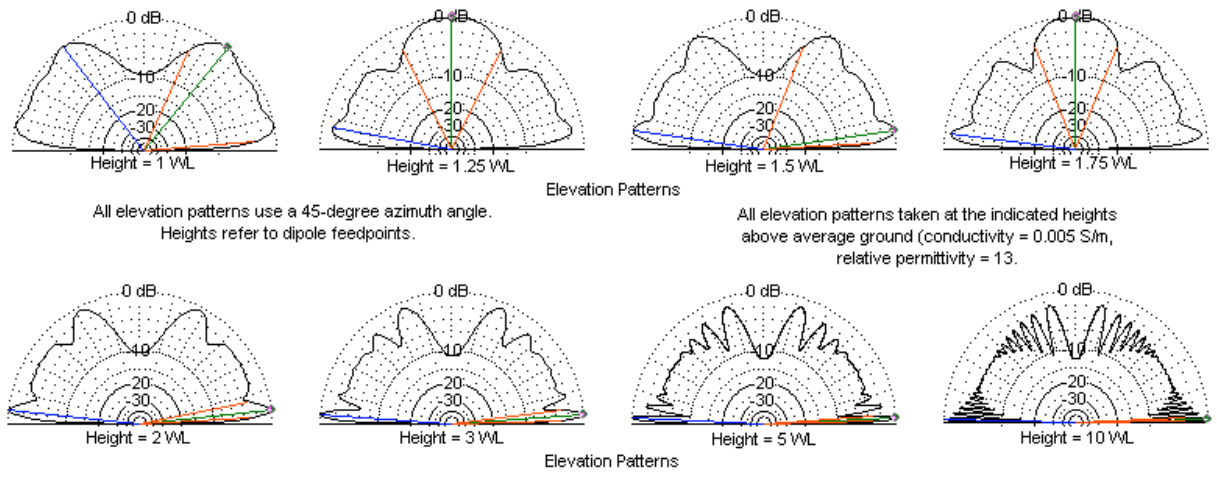

Sample Total-Field Patterns of an "Up" Lindenblad Antenna

Fig. 11

Even though the modified Lindenblad provides superior low elevation angle performance, the array has limits in terms of the height at which we should position it. Note that the lowest elevation lobe begins to dominate by a height of 2 λ above ground. At heights of 5 λ and upward, the lobes and nulls at very low angles become serious phenomena. Although 3-5 λ is an appreciable height for a 2-meter antenna, the same height in wavelengths may not be sufficient at 70 cm to clear ground clutter. Hence, for all of its other virtues, the modified Lindenblad remains subject to the same pattern formation influences that informed the patterns of the other candidate antennas. (However, the lobe development is severely retarded relative to the original design.)

Of all the candidates for a fixed-position satellite antenna in our survey, the modified Lindenblad achieves the best low angle performance, where we understand "low angle" to mean a range of angles in the sky that a satellite is likely to traverse. (We must set aside some of our HF antenna ideas to grasp the needs of satellite communications.) Between 10° and about 50° elevation, no other candidate achieves an equivalent evenness of gain. For angles from about 30° up and higher across the sky, the turnstiled Moxon rectangles take honors among the candidates in the survey. Still, no single antenna type achieves

the ideal of a dome across the sky with equal gain in every possible direction and at every possible height.

The survey has not been all-inclusive. It has featured some historically important first attempts at usable satellite antennas adapted from omni-directional terrestrial antennas. It finished with two more recent entries, one geared toward smooth higher-angle gain, the other designed 60 years ago for lower elevation angles. In all of the exercises, we have seen that height above ground presents the fixed-antenna user with a conundrum. Greater antenna heights clear the ground clutter, but produce considerable numbers of lobes and nulls. Lower heights tend to clean up the pattern, but may block lower elevation angles due to intervening structures, both man-made and natural. Unless we have specific interests that allow a simple fixed antenna to serve us well, eventually, we shall begin to look at antennas that we can aim and that are worth aiming. We may begin with simple hand-held antennas that we point from our patios. Even while claiming total satisfaction with simplicity, we keep on checking the prices of Az-El rotator systems and dreaming of long-boom antennas with high gain and narrow beamwidths.

Aimable Highly Directional Antennas

One solution to virtually all forms of DX and off-world communications at VHF and UHF is the use of highly aimable antennas using azimuth and elevation rotators under computer control. However, the needs of EME and of satellite communications differ. The moon is a relatively large target, but requires the highest available antenna gain, since it is a passive and not very efficient reflector. Satellites are small objects (in terms of arc-seconds of diameter), but require controlled lower gain values to prevent overloading their inputs. Therefore, we shall divide our discussion into two parts, one for very long-boom antennas and the other for circularly polarized antennas using conventional techniques. However, we shall (for the moment) confine ourselves to the total far field radiation pattern and reserve polarization matters for the third part of this review.

1. *A Very Long Boom Horizontally Polarized Yagi*: For EME work, the most common antenna is the very long-boom Yagi used singly or in arrays or 2, 4, or more. Since our goal is to look at what happens to a Yagi pattern when we tilt the antenna at various elevation aiming angles, we may sample the field with a single representative. The antenna that I have selected uses a 13.25-λ boom. In DL6WU and similar long-boom Yagi designs, this boomlength would accommodate about 39 elements, but the present special design uses 50 elements. For more exacting physical and performance details of this 432-MHz antenna, see *Long-Boom Yagi Studies*. **Fig. 12** shows the outline of the antenna, along with free-space E-plane and H-plane patterns. The figure also provides essential free-space performance data for quick reference. The most notable performance feature of the antenna is that it attenuates both E-plane and H-plane sidelobes by at least 24 dB relative to the main forward lobe. Typical values for antennas that use a similar boomlength and produce about the same forward gain are 15 to 17 dB.

Before we put the antenna through its paces, let's pause to examine one of those sound bites that infect amateur radio antenna studies. For horizontal antennas over ground, we find an oft-quoted equation for determining the elevation angle (α) of the first lobe of an antenna pattern:

$$\alpha = \sin^{-1}(1/4H)$$

H is the height of the antenna above ground in wavelengths. If we place the antenna 1 λ above ground, the calculations say the value of α is 14.5°. Although ground quality plays some role in modifying the results of the simplified calculation (that assumes perfect ground), the equation seems to work fairly well for dipoles. A modeled dipole 1 λ over average ground shows an elevation angle for its first lobe of 14°. We may also note that the free-space gain of this 300 MHz aluminum dipole is 2.11 dBi. 1 λ over average ground, the maximum dipole gain is 7.57 dBi. Ground reflections add 5.46 dB to the free-space gain value.

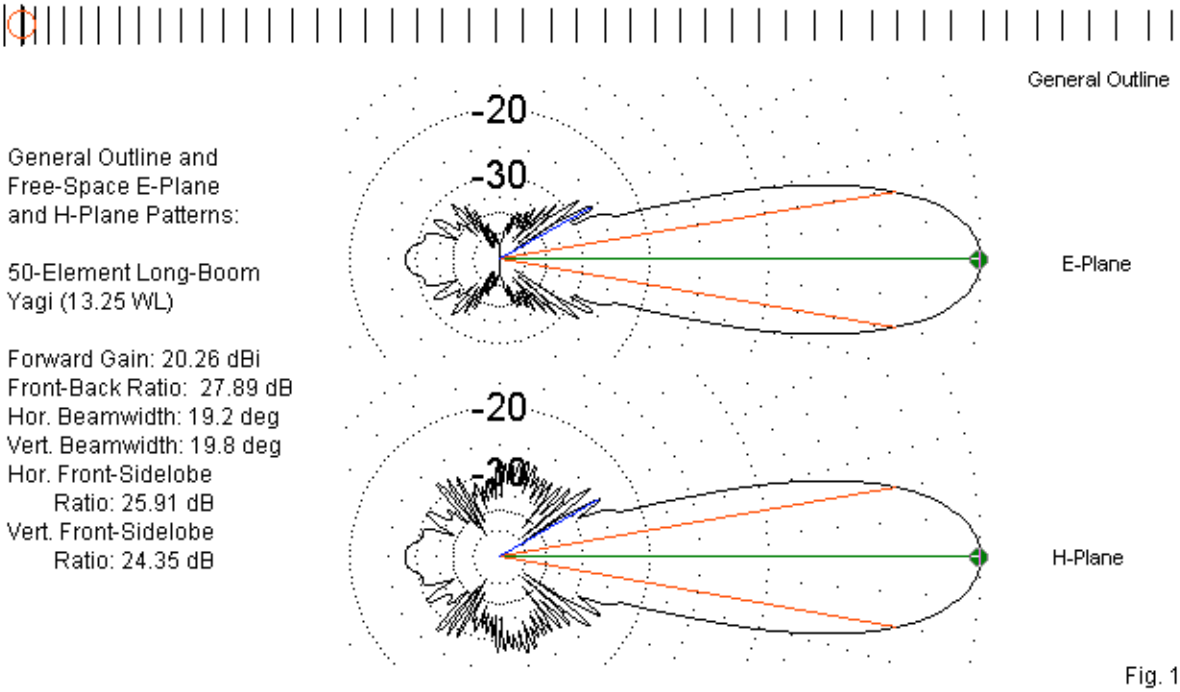

Fig. 12

Unfortunately, we carry both simplified bits of information into all of our antenna planning. While we have a long-boom, high-gain Yagi at our disposal, let's place it 1 λ above average ground in a position parallel to the ground. The model shows the maximum forward gain as 22.77 dBi with a main lobe elevation angle of 9°. Both results (only +2.5-dB added gain and -5° elevation) are anticipated and normal. As we increase the forward gain and the boom length of an antenna, the additional gain provided by ground reflection decreases steadily at low heights. When moving from a dipole to Yagis as short as 8 elements, we may lose a full dB from the peak value of ground-reflection gain additions. As well, over that same span, the elevation angle decreases by over a degree. The results for our very long-boom Yagi simply carry out the progression to greater extremes. As we raise the antenna to greater heights, some of the added ground-reflection gain emerges. However, when designing a long-boom Yagi, do not carry over small-antenna rules of thumb. They require extensive modifications that do not lend themselves to sound-bite treatment.

Our main goal in using the long Yagi is to see what happens when we gradually tilt it higher into the sky. Since the boom is so long, I shall presume that we mount the antenna at its center. To prevent the reflector from intercepting the ground, I selected a mounting height of 7.5 λ. That height allows me to tilt the antenna straight upward and still clear the ground by nearly 1 λ. To provide a relatively complete catalog of patterns, I checked the antenna at 15° intervals. **Table 6** shows the data collected for this series of modeling exercises. El angle indicates the reported angle of maximum radiation. Hor BW and Ver BW are the reported horizontal and vertical beamwidths. Hor FSL and Ver FSL indicate the horizontal and vertical front-to-sidelobe ratios.

The table alone provides some interesting information about what happens to a radiation pattern as we tilt the antenna ever higher. First, the elevation angle of maximum radiation may not correspond precisely with the aiming angle. In this case, the differences are slight, but that should not be a universal presumption. Second, at a 0° tilt angle, we find the additional gain supplied by ground reflections (higher now that we are 7.5 λ high), but as soon as we tilt the antenna to 15°, we lose the ground-reflection gain advantage. All other gain values are very close to the free-space gain value. Third, the vertical front-to-sidelobe ratio shows an expected low value, at 0° tilt, since we know that at a height of 7.5 λ, we shall find many elevation lobes. At 15° tilt-angle and higher, we lose the ground-induced elevation lobes and nulls

as clear and distinct phenomena. However, they still have an affect on the pattern in the form of ripples. At some angles (for example, 15° and 60° in this exercise), the ripples may be strong enough to show up as distinct lobes in NEC software. However, if you examine the elevation patterns in **Fig. 13**, you will see (even in the small-scale patterns) that the forward lobes are not nearly as smooth as the main H-plane lobe in the free-space patterns.

Table 6. Performance of a 50-Element, 13.25-λ Long Yagi at 7.5 λ Center Height above Ground Using Stepped Tilt Angles

	El Angle (degrees)	Gain (dBi)	Front-Back Ratio (dB)	Hor BW (degrees)	Ver BW (degrees)	Hor FSL Ratio (dB)	Ver FSL Ratio (dB)
Reference Data							
Free Space	---	20.26	27.89	19.2	19.8	25.91	24.35
0° Tilt, 1 λ Height	9	22.77	28.27	18.0	9.4	23.24	24.80
Tilt-Test Data							
Tilt Angle (deg)							
0	1.9	26.11	27.91	19.2	1.4	25.82	0.95
15	14.5	20.69	34.67	20.2	17.9	21.70	0.49
30	29.1	20.47	30.69	22.4	19.5	22.76	19.48
45	45.4	20.48	25.66	27.8	19.1	23.18	21.86
60	57.8	20.31	26.75	37.4	19.3	24.09	0.06
75	75.0	20.20	22.07	75.9	19.9	22.07	21.64
90	90	20.20	---	20.0	20.0	22.51	21.65

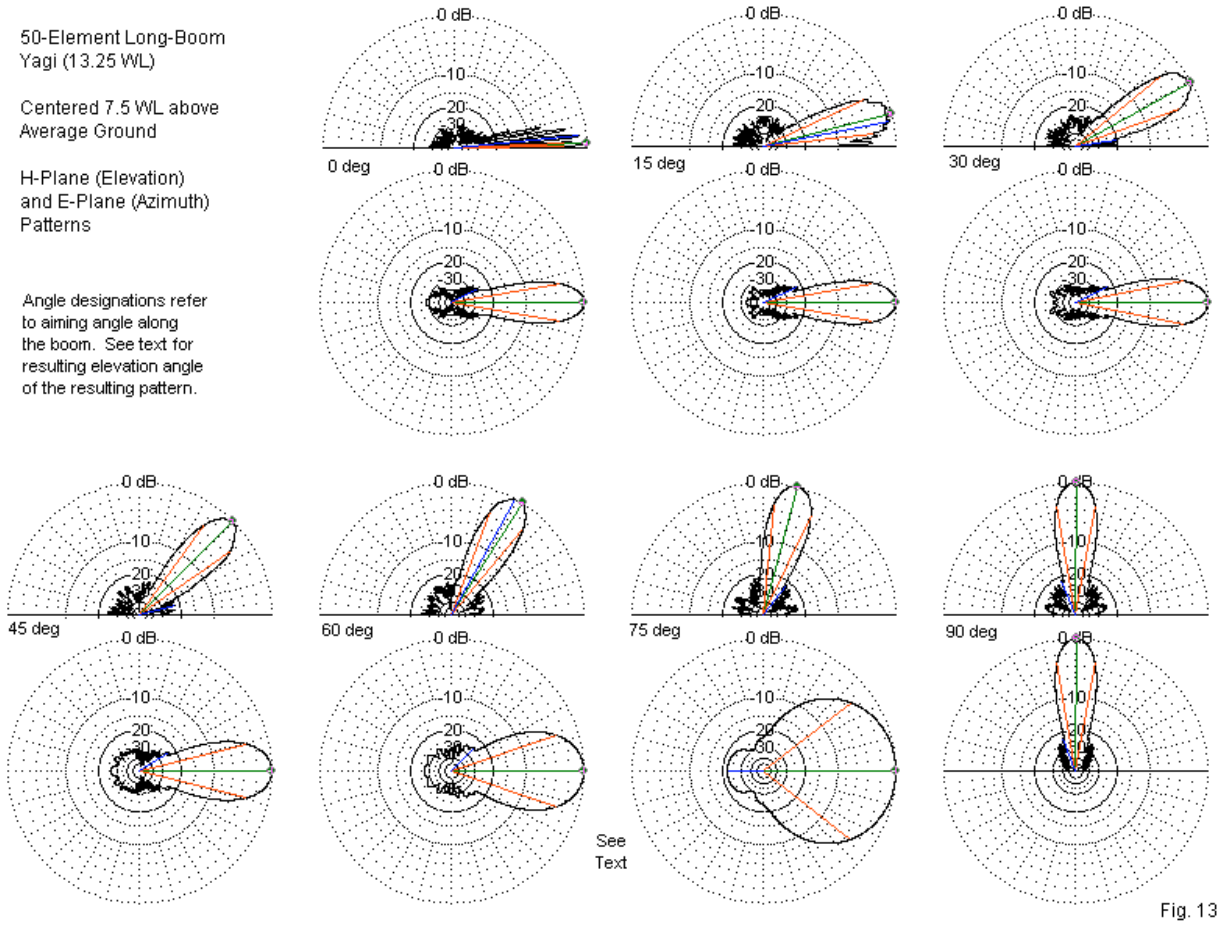

Fig. 13

One reason for my use of the selected long-boom Yagi is that it allows us to focus on main-lobe behavior without strong forward and rearward sidelobes interfering with the data. You may note that the final azimuth pattern is not a conventional pattern. Instead it is an elevation pattern with the axis shifted 90° to capture the E-plane radiation field of the antenna. However, both the other azimuth patterns and the tabular data seem to present a problem, namely, a sudden reduction in the horizontal beamwidth of the antenna between a tilt of 75° and a tilt of 90°.

The apparent results are an illusions bred of one necessity in 2-dimensional pattern generation on a polar plot. As we increase the plot's elevation angle, we are actually sampling data from the surface of a cone and transferring it to the circle at the top of the cone. Essentially, at very high tilt angles, only the peak gain data is an accurate graphical representation of the pattern. All other distances undergo foreshortening. From tilt angles of about 45° through 75°, foreshortening increases the apparent width of the pattern, while the pattern itself has not changed its beamwidth by any significant amount. To show the general state of the patterns at high tilt angles, **Fig. 14** presents three 3-dimensional patterns for the antenna for tilt angles of 60°, 75°, and 90°. Fine detail is not apparent in these plots, since they use a 5° increment in sampling steps (to avoid patterns that are mere black blobs). However, the relative consistency of the horizontal and vertical beamwidths is clearly evident.

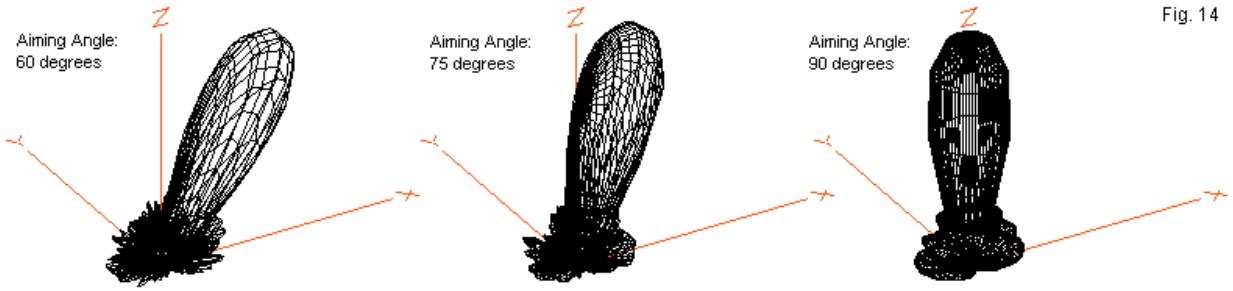

Fig. 14

3-Dimensional Patterns of a 50-Element Long-Boom Yagi at High Elevation Angles

The results that we obtained for the 50-element Yagi on a 13.25-λ boom apply to virtually any other high-gain Yagi that we might use for EME communications. If we lower the gain, then beamwidths will necessarily broaden. The higher level of sidelobes in some designs of the same boomlength and gain may narrow the beamwidth by up to 2°. Those same sidelobes may also increase the temperature of the antenna and hence limit the signal-to-noise ratio or make the antenna susceptible to off-axis signals or noise. Nevertheless, the subject beam does provide a compendium of data that is useful in planning an EME installation, at least in terms of reasonable expectations that we may carry to our EME antennas.

When we turn to aimable satellite antennas, we generally employ arrays with far lower gain levels and far shorter booms. We shall sample a few representatives that have one feature in common: they are all circularly polarized. In fact, the models use right-hand circular polarization. For the moment, this fact lies in the background, since we shall explore only the total-field patterns. Because all of these antennas have short booms, it will be convenient to set the rearmost elements at 7.5 λ and let the boom extend upward from the point. I shall also reduce the number of steps in the tilt tests to include only 0°, 45°, and 90°.

2. *A 4-Element Circularly Polarized Quad Beam*: A circularly polarized quad beam shows only one difference relative to a quad beam that is linearly polarized. From the common feedpoint at one corner of the driven loop, a ¼-λ (or a ¾-λ) line will run to an adjacent corner. The outline sketch in **Fig. 15** shows the line. To switch from left-hand to right-hand polarization (and back) only requires that we feed the driven element at the correct corner. The sample quad beam in the sketch uses 4 elements with a 0.91-λ boom. The largest dimension is 0.27-λ per side. **Table 7** provides the relevant performance data for the array through the truncated tilt tests.

Table 7. Performance of a 4-Element, 0.91-λ Long Quad Beam at 7.5 λ Base Height above Ground Using Stepped Tilt Angles

	El Angle (degrees)	Gain (dBi)	Front-Back Ratio (dB)	Hor BW (degrees)	Ver BW (degrees)	Hor FSL Ratio (dB)	Ver FSL Ratio (dB)
Reference Data							
Free Space	---	10.12	20.95	60.5	60.6	16.61	15.96
Tilt-Test Data							
Tilt Angle (deg)							
0	1.9	15.60	21.06	60.1	1.9	16.43	0.91
45	44.4	10.66	18.86	87.6	53.4	16.46	0.08
90	90	10.51	---	57.0	57.2	1.19	1.19

The free-space performance is the benchmark against which we evaluate the performance over ground. At a 0° tilt-angle and a height of 7.5 λ, we find the ground reflection gain, but the multiplicity of elevation lobes supplies the vertical beamwidth value. Above 0° tilt, we lose the ground reflection gain. More surprisingly, we do not find the (free-space) normal vertical beamwidth, as we did with the very long-boom Yagi. Instead we find a very large angle. Unlike the large horizontal beamwidth that we can attribute to pattern foreshortening on the polar plot, the vertical beamwidth angle is a true rendition of the pattern. Note in **Fig. 15** that the inner pattern of null-depths traces the normal (free-space) H-plane beam, but a series of lobes project to much greater strength. As well, the pattern shows a very high ripple content and therefore yields numerous secondary gain peaks. The result is a very small vertical front-to-sidelobe ratio. Allowing for the foreshortened 45°-azimuth pattern shape, the azimuth performance of the antenna is normal at every tilt angle.

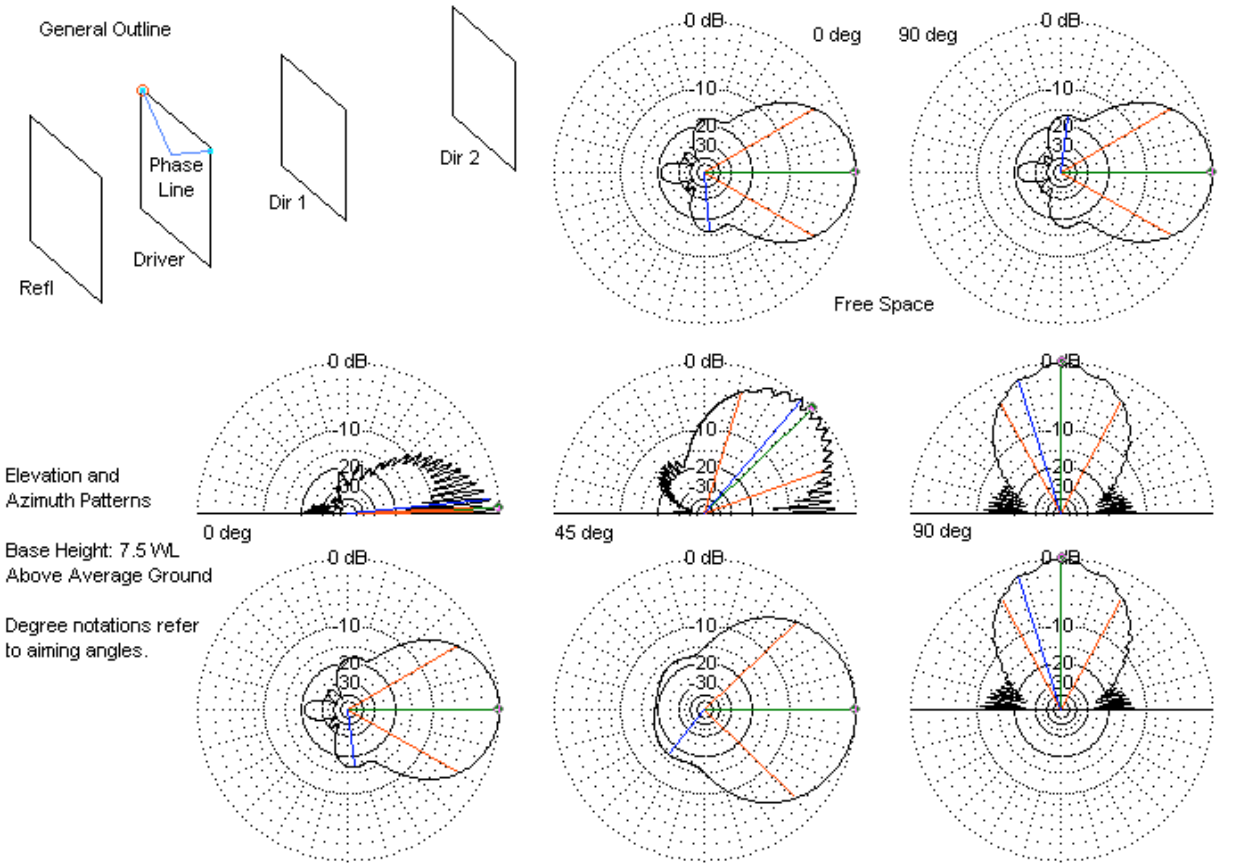

General Outline and Sample Patterns at Selected Angles
4-Element Turnstile Quad Beam

Fig. 15

The circularly polarized beam is nevertheless quite adequate for many satellite communications needs, if we assume that low elevation angles do not unduly increase noise reception. However, the quad leaves us with a question: does the 45°-elevation performance result from the circularly polarized construction or from the relatively low gain and high beamwidth of the antenna?

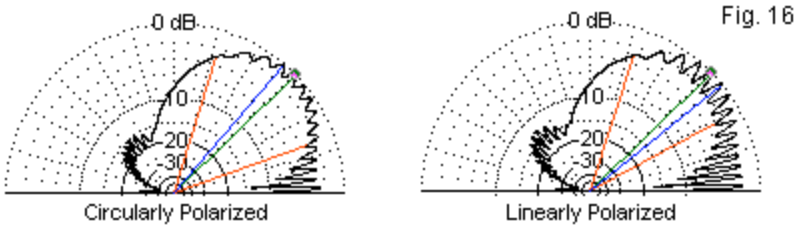

Fig. 16

45-Degree Tilt Elevation Patterns of a 4-Element Quad Beam
Using Circular and Linear Polarization Feed Systems

Fig. 16 provides the answer. I simply removed the phasing line from the original model and moved the feedpoint to the center of the horizontal wire between the phase-line corners. The pattern for this version of the antenna, still tilted 45° relative to the ground, is a pattern that has the same properties as the original circularly polarized version of the antenna. Without the circularly polarizing feed system, the pattern shows a greater ripple content with slightly stronger (about 0.7 dB) peaks and equally deeper nulls. It would appear that the elevation pattern shape is a function of basic array gain. The following circularly polarized Yagis have slightly higher basic gain values and may shed more light on the applicable trends for 45° tilt elevation patterns.

3. *A Circularly Polarized 8-Element Yagi with Crossed Elements*: Our first Yagi is a circularly polarized 8-element array on a 1.42-λ boom. It uses crossed elements so that all parasitic elements meet at their centers. The drivers provide just enough separation to allow the installation of a ¼-λ phasing line. The longest elements are 0.47 λ. The array uses "fat" elements, that is, 12.7-mm (0.5") diameter aluminum tubes. **Fig. 17** shows the beam outline and the free-space patterns in the upper portion of the figure. Since the antenna is a NEC model, it assumes the use of a non-conductive boom or elements that are well insulated and isolated from a conductive boom. We should also note in passing that, when we label one of these aimable antennas as a circularly polarized array, the label only means the antenna is set up for circular polarization. It does not indicate the degree to which the antenna achieves such polarization.

As the free-space patterns reveal, the antenna has not been optimized to eliminate sidelobes. Those same sidelobes appear in various ways in the patterns taken over ground. I have left them to see what happens when we place the beam vertically at a height of 7.5 λ above ground. **Table 8**, in conjunction with the lower portion of **Fig. 17**, shows the performance of the beam at various tilt angles. The basic gain of the array is about 2 dB higher than the quad beam, and this value shows up at all angles. The seemingly small increment of gain has a considerable effect on the 45°-tilt pattern, with a very significant reduction in very-low-angle gain. In contrast to the relatively clean quad forward lobe at a 90° tilt, the Yagi shows as many or more ripples than at a 45° tilt.

Although the graphs do not show as many tilt angles as we used for the 50-element Yagi, the 45° pattern still shows evidence of cone-to-circle foreshortening. In general, the actual horizontal beamwidth for antenna that we have aimed at an angle above the horizon answers approximately to a simple equation:

$$BWa = BWr \cos \alpha$$

BWa is the actual beamwidth, BWr is the beamwidth reported by NEC, and α is the aiming elevation angle of the antenna.

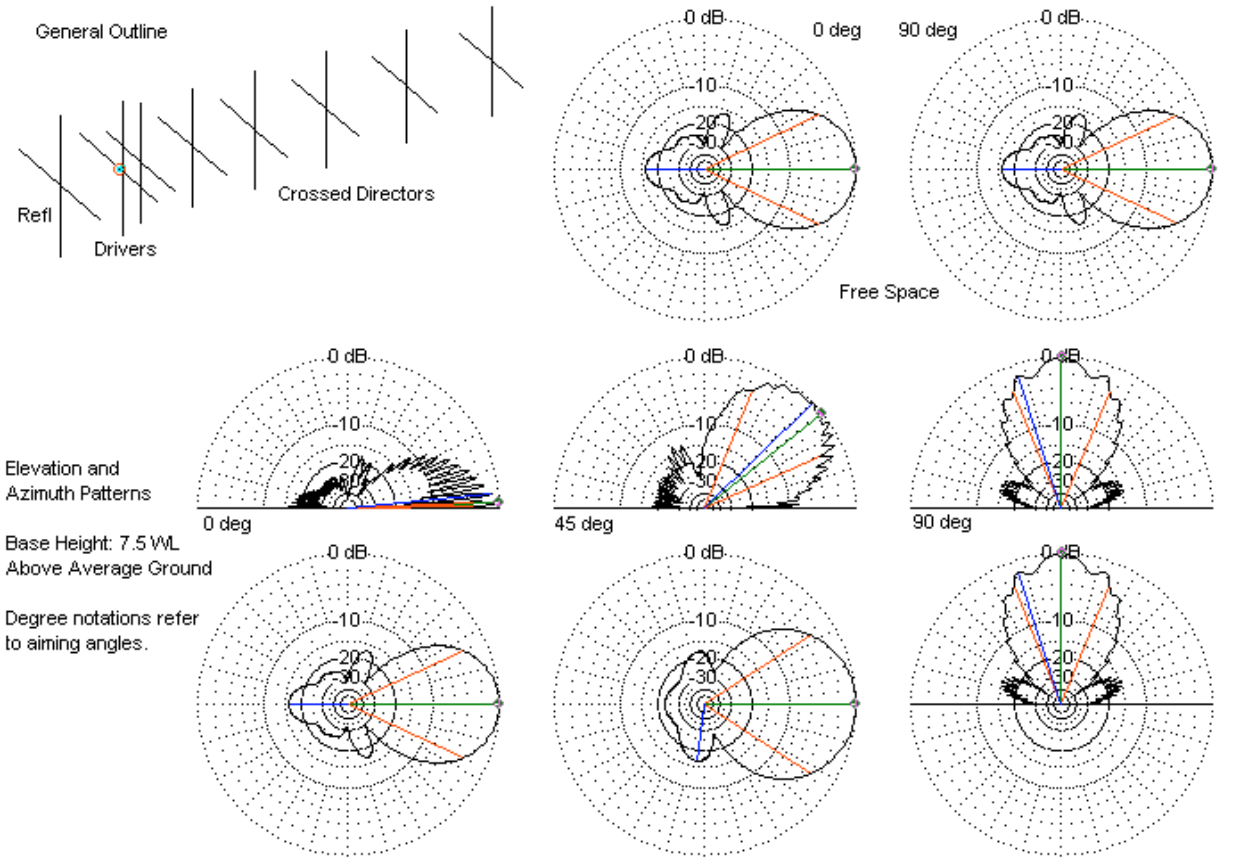

General Outline and Sample Patterns at Selected Angles
8-Element Turnstile Yagi with Crossed Elements

Fig. 17

Table 8. Performance of an 8-Element, 1.42-λ Long Yagi at 7.5 λ Base Height above Ground Using Stepped Tilt Angles

	El Angle (degrees)	Gain (dBi)	Front-Back Ratio (dB)	Hor BW (degrees)	Ver BW (degrees)	Hor FSL Ratio (dB)	Ver FSL Ratio (dB)
Reference Data							
Free Space	---	12.01	15.94	50.2	51.0	15.94	15.94
Tilt-Test Data							
Tilt Angle (deg)							
0	1.9	17.53	15.96	49.8	1.9	15.95	0.85
45	39.0	12.20	22.66	66.2	44.4	16.58	0.03
90	90	12.58	---	44.6	44.8	1.41	1.36

Except for the foreshortened 45°-azimuth pattern, the antenna over ground suggests a narrower horizontal beam angle than in free space. Despite the ripples in the pattern, the 8-element Yagi would provide relatively good aimed satellite service in a small package that one might support from the rear end in UHF arrays.

4. *A Circularly Polarized 12-Element Yagi with Crossed Elements*: The 12-element Yagi on a 2.61-λ boom is essentially an extended version of the 8-element Yagi. It uses the same layout and feeding system. The upper portion of **Fig. 18** shows the general outline and free-space E-plane and H-plane patterns. The longer boom doubles the number of forward sidelobes, since that number is generally the same as the boomlength's integer. However, the front-to-sidelobe ratios for both planes are similar to the values for the 8-element Yagi.

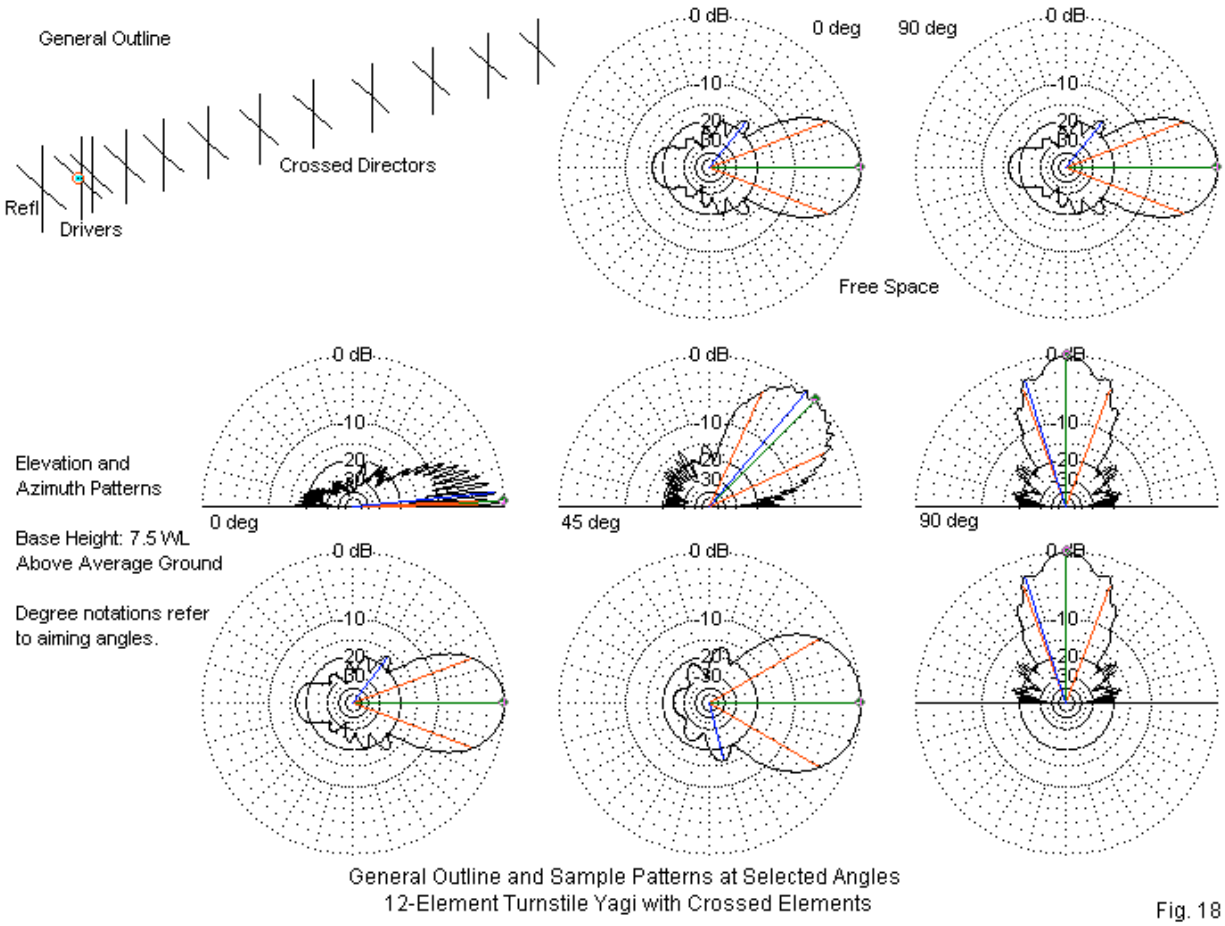

General Outline and Sample Patterns at Selected Angles
12-Element Turnstile Yagi with Crossed Elements

Fig. 18

Table 9. Performance of a 12-Element, 2.61-λ Long Yagi at 7.5 λ Base Height above Ground Using Stepped Tilt Angles

	El Angle (degrees)	Gain (dBi)	Front-Back Ratio (dB)	Hor BW (degrees)	Ver BW (degrees)	Hor FSL Ratio (dB)	Ver FSL Ratio (dB)
Reference Data							
Free Space	---	13.49	16.53	42.2	42.4	16.15	16.07
Tilt-Test Data							
Tilt Angle (deg)							
0	1.9	18.99	16.55	41.8	1.9	16.42	0.91
45	45.0	13.70	24.12	61.3	40.6	15.97	0.06
90	90	14.15	---	41.2	41.2	2.05	2.02

Despite adding over a wavelength to the boom, we net a gain increase of about 1.5 dB for all tested conditions. The added gain does result in a beamwidth reduction in both planes. Notice especially the increased control of the lower angles of the 45°-tilt elevation pattern. Accompanying the improvement in the low-angle radiation for the 45°-levation pattern is an increased ripple factor in the patterns, especially at 90°. Although the pattern appears somewhat messy, that fact is no hindrance to the use of the antenna as an aimed array for overall sky coverage. We shall explore in the last part of these notes whether or not the ripples have an adverse affect on the circular polarization of this antenna.

5. *A Circularly Polarized 10-Turn Axial-Mode Antenna*: Numerous amateur builders have attempted to popularize the axial-mode helix as a satellite antenna. Most such antennas have emerged from

generalized graphs, without adequate study of how these antennas perform in relatively narrow-band amateur service. The subject antenna will use 10 turns with a 1.15-λ circumference and a 12° pitch. As well, it will use a 1.2-λ by 1.2-λ rear screen. If you re-read last year's contribution to the *Proceedings of the Southeastern VHF Society* ("Notes on Axial-Mode Helical Antennas in Amateur Service"), you will find that these dimensions are close to optimal for the number of turns in the helix. The overall boomlength is 2.52 λ, including the screen at the rear. The top portion of **Fig. 19** shows the general outline of the helical beam, along with the free-space patterns. The critical performance data for the modeled test conditions appear in **Table 10**.

Table 10. Performance of a 10-Turn Axial-Mode Helix at 7.5 λ Base Height above Ground Using Stepped Tilt Angles

	El Angle (degrees)	Gain (dBi)	Front-Back Ratio (dB)	Hor BW (degrees)	Ver BW (degrees)	Hor FSL Ratio (dB)	Ver FSL Ratio (dB)
Reference Data							
Free Space	---	12.44	15.13	30.3	30.2	8.80	9.49
Tilt-Test Data							
Tilt Angle (deg)							
0	1.8	17.90	15.08	30.2	1.9	8.97	1.09
45	39.3	12.88	15.74	40.9	24.9	9.23	0.09
90	83/98	11.96	---	31.7	31.9	5.93	6.07

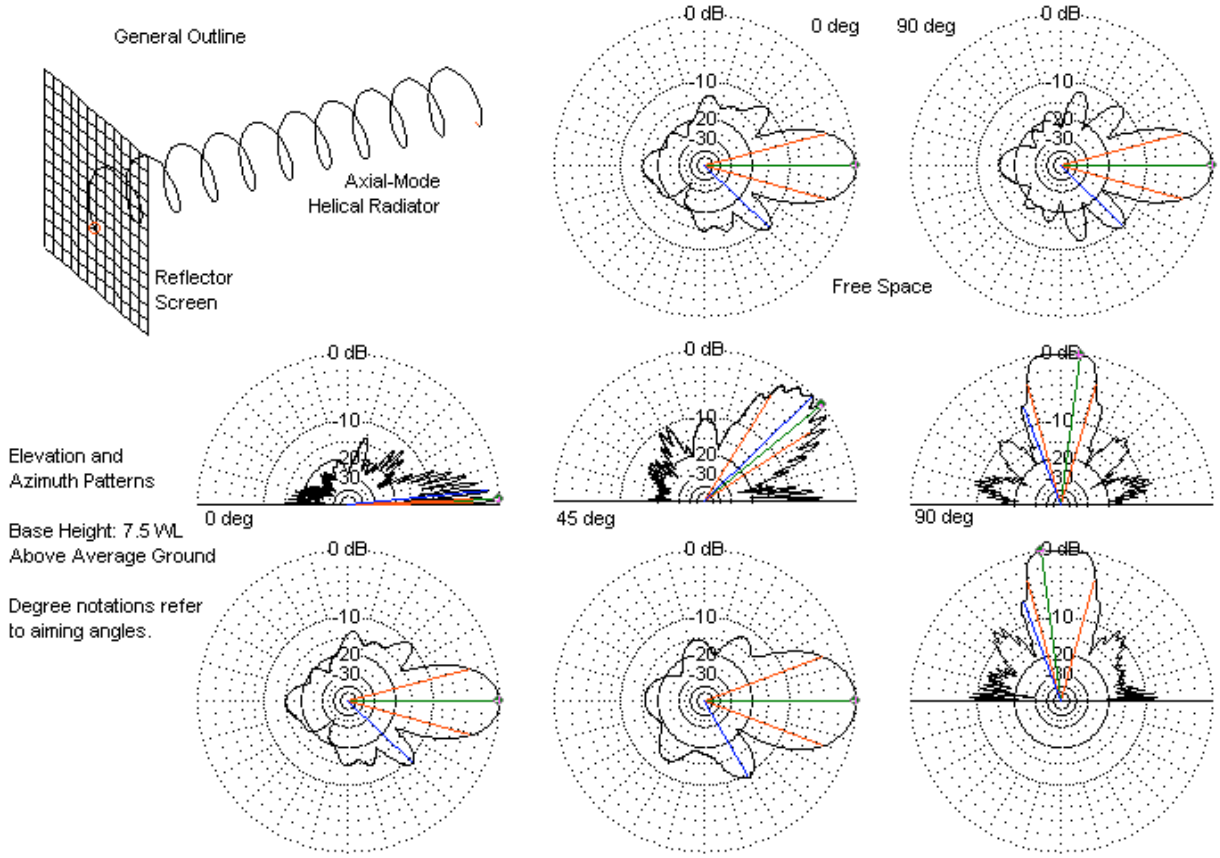

General Outline and Sample Patterns at Selected Angles
10-Turn, 1.15-WL Circumference, 12-Degree Pitch Axial-Mode Helical Radiator

Fig. 19

The tabular data show a number of interesting properties that become striking in contrast to the 2 circularly polarized Yagis. The gain levels are in between the values of the Yagis and closer to the value

of the 8-element version, although the virtual boomlength is about equal to the longer Yagi. Despite the gain level, the axial-mode helix shows lower beamwidth values (by about 10°) than the longer Yagi.

The elevation angle for the antenna, when aimed straight up, is not 90°. Instead, we find two values due to the fact that the forward lobe is beginning to split into two peaks. The values are not equal amounts away from 90 degrees because an axial-mode helix is not symmetrical about its centerline. The rearmost turn, which is also the feed turn, makes contact with the screen, which disturbs perfect performance symmetry, no matter how perfectly we physically construct the antenna. See the 90° patterns in **Fig. 19**. The absence of symmetry in an axial-mode helix results in some significant pattern aberrations, relative to what we might normally expect. The azimuth patterns show unequal sidelobe development. In addition, the 45°-tilt elevation pattern shows considerable low-angle radiation (or reception sensitivity, which might suggest an even stronger disadvantage). Sidelobe attenuation is mediocre at best. It is possible to use smaller circumference values to achieve a cleaner pattern, but the cost is a considerable loss of gain at a small decrease in the virtual boomlength.

For aimed service, the axial-mode helix may not live up to its reputation, which has been garnered from inadequate study of the antenna's actual performance. Indeed, the axial-mode helix originated as a wide-band antenna with moderate performance. Use of the antenna for aimed satellite service is certainly possible, although the crossed-Yagi designs have superior performance values. By a length of 10 to 12 elements (or about 1.8 to 2.5 λ of boom), the low-angle radiation with a 45° tilt has diminished to relatively inconsequential levels. The wider-beamwidth may ease the problem of satellite acquisition and lock. Of course, we may always design better Yagis with crossed elements than the samples that we are using here. In the process, we might easily reduce the sidelobe strength and improve the basic front-to-back level. We may also increase gain by adding more elements. For our purposes, the samples--with all of their shortcomings--will suffice.

Nevertheless, some important questions remain. Primary among them is how well the crossed Yagis achieve circular polarization in comparison to the apparent inherent circular polarization of the axial-mode helix. Answering that question will inevitably lead us back to the basics of polarization and to how vertical and horizontal polarization are related to circular polarization. No wonder that I have set aside an entire section of these notes for the subject.

Circular Polarization

Understanding circular polarization involves several facets of antenna data to which radio amateurs normally do not pay attention. Much of it fails to appear in most antenna handbooks, although it does appear in various places in introductory college texts. If we do some antenna modeling, we have access to the data, but rarely do we pay much attention to it. NEC (both -2 and -4) provide most of the necessary data to understand circular polarization in the radiation pattern section of the tabular output report.

To capture some of the essential information and its meaning, let's examine just one line of a typical output-report radiation-pattern table. The model happens to be a 5-turn right-hand axial-mode helix placed over perfect ground, and the line is for an elevation pattern at the zenith or overhead angle.

```
                         - - -  RADIATION PATTERNS  - - -

  - - ANGLES - -           - POWER GAINS -       - - - POLARIZATION - - -
THETA     PHI         VERT.    HOR.      TOTAL      AXIAL      TILT   SENSE
DEGREES   DEGREES       DB       DB        DB        RATIO      DEG.
 0.00     90.00       10.39     3.84    11.261     0.46544     -3.89  RIGHT

           - - - E(THETA) - - -       - - - E(PHI) - - -
          MAGNITUDE      PHASE      MAGNITUDE      PHASE
            VOLTS       DEGREES       VOLTS       DEGREES
          1.00721E+00   -99.56      4.73544E-01    163.94
```

The first 2 entries are the angles, called theta and phi. Theta angles correspond to elevation angles, but count downward from overhead. Hence, the elevation angle is 90-0 = 90°. Phi angles correspond to azimuth angles, but increase counterclockwise. True azimuth or compass-rose angles count clockwise. Hence, the azimuth angle shown would be 360-90 = 270°. Essentially, NEC emerged from the work of physicists and strict Cartesian coordinate users, not from field engineers.

The next 3 entries list the power gains in dBi for the total field, the one that we have shown for all antennas so far, along with the vertical and horizontal components of that gain. Note that we cannot simply add up the power gain of the components to arrive at the total far-field gain. Instead, we must convert the individual component power gain values in dB back to simple power ratios in accord with the basic equation for calculating power gain in dB.

$PG_{dB} = 10 \log_{10} (P1/P2)$

P2 will always be 1, since NEC calculates in terms of dBi, and an isotropic radiator has a power gain of 1 and hence a power ratio of 1/1. So we may obtain a value for the power ratio using the reverse form of the equation:

$P1/P2 = \log^{-1}_{10} (PG_{dB}/10)$

The conversion of the vertical component gain yields 10.94 (with no units, since the power ratio is dimensionless). The conversion of the horizontal component yields a ratio of 2.42. If we add these values, we obtain 13.36, and we may re-convert this number back into a power gain in dBi. If we let the subscripts stand for the vertical and horizontal power ratios, respectively, the relevant equation is very straightforward.

$PGT_{dB} = 10\log_{10} (P1_a/P2_a + P1_b/P2_b)$

The result is 11.26 dBi, the total gain shown in the line from the table.

Most radiation table-readers stop at this point. However, the remaining entries are critical to understanding circular polarization. The table lists the axial ratio, the tilt angle, and the sense of polarization. We have an inkling of understanding of the "sense" entry, since we initially specified that the helix model was right-handed. So we sort of expect right-hand polarization. However, for most amateurs, the remaining entries are a bit of a mystery. Although the following explanation is woefully short of being complete, it may at least orient you to the general subject of polarization in antenna work. **Fig. 20** will be our focal point.

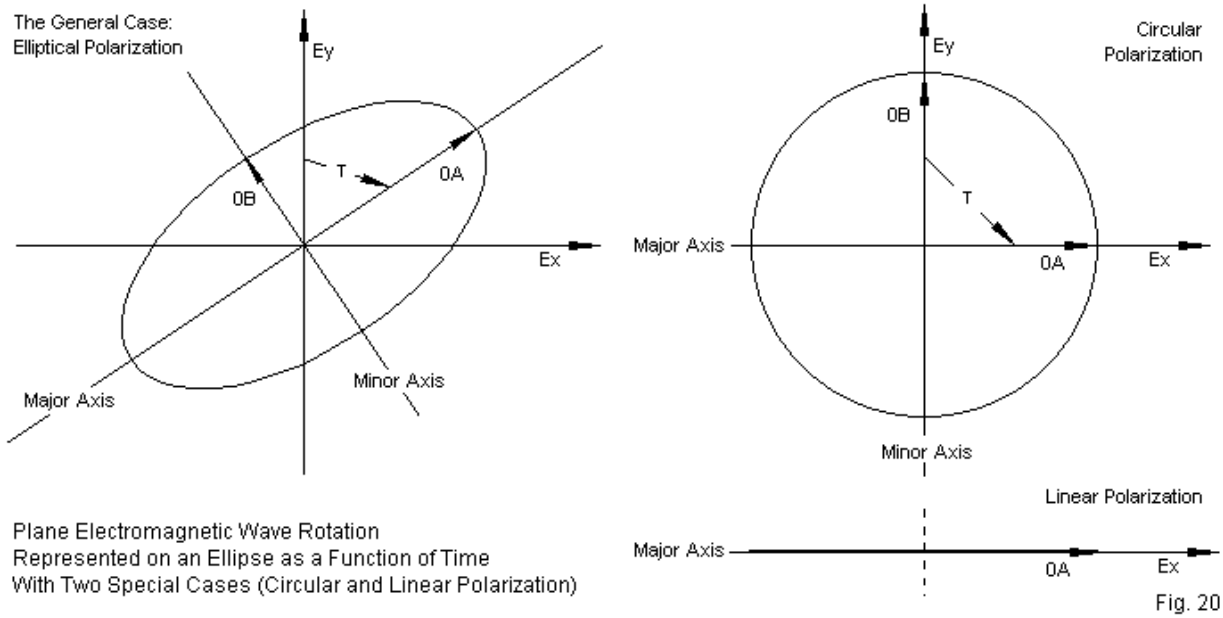

Plane Electromagnetic Wave Rotation
Represented on an Ellipse as a Function of Time
With Two Special Cases (Circular and Linear Polarization)

Fig. 20

The oval on the left is a means of representing the rotation of a plane electromagnetic wave when referred to a central point and tracked in time--very tiny increments of time. The figure forms an ellipse, and every possible form of polarization of plane waves forms some variation of an ellipse. Every ellipse

has a long or major axis and a short or minor axis. For a given situation, these axes may or may not align with the graph axes--and in most cases do not. Hence, relative to the Y-axis, the major ellipse axis forms an angle, τ, the tilt angle in the line from the radiation table. NEC likes to count the size of all its angular quantities in terms of +180° to -180°. Textbooks (for example Balanis, *Antenna Theory: Analysis and Design*, 2nd Ed. (Wiley, 1997), pp. 64-73) like to calculate the axial ratio this way:

AR = Major Axis/Minor Axis = 0A/0B

This method gives the axial ratio a possible range of 1 to infinity. To confine the numbers, NEC reverses the equation:

AR = Minor Axis/Major Axis = 0B/0A

The result is equally valid, but the number range is now from 1 down to nothing.

If the major and minor axes are identical in strength, as in the top-right part of **Fig. 20**, then we obtain perfect circular polarization. Rarely is a radiation pattern in any direction so perfect that 0A and 0B are exactly equal. Even if we find the same numbers carried to 2 decimal places being identical, the circle may have a very tiny elliptical shape. So for nearly perfect circular polarization entries, expect almost any value for the angle. Quite frankly, even nearly perfect circular polarization is very rare in antennas. Perfectly circular polarization would have an AR value of 1.0. Our sample helical antenna, held in high regard among amateurs for its circular polarization, manages only an AR value of 0.465. Those who absolutely must have circular polarization in the antenna industry have gone to bifilar and quadrifilar helical windings in their efforts to overcome the shortcomings of our simple monofilar helices.

If we have only a single component or if we have two components that are essentially in phase or exactly 180° out of phase, then we obtain the crushed ellipse of the lower right corner in **Fig. 20**. This situation yields linear polarization, and it is quite common. NEC may show the tilt angle in such cases as 0°, 90°, or -90°, depending on its internal conventions of substituting values for vanishing quantities. However, the tilt angle becomes largely irrelevant for linearly polarized elements and antennas. The critical quantity is the axial ratio, which is zero. Actually, NEC will call polarization linear wherever the major axis value is many orders of magnitude larger than the minor axis.

To illustrate what we might obtain by way of a radiation pattern report for a linearly polarized antenna, I took a simple 3-element Yagi, pointed it straight upward and placed the reflector 1 λ above average ground. **Table 11** provides a truncated glimpse at the radiation pattern, since I limited the sample to every 10° of elevation. Also, note the theta convention for elevation angles: 0° is over head and 90° is the horizon.

Table 11. 3-Element Yagi Pattern Data

- - ANGLES - -		- POWER GAINS -			- - - POLARIZATION - - -			- - - E(THETA) - - -		- - - E(PHI) - - -	
- - - RADIATION PATTERNS - - -											
THETA	PHI	VERT.	HOR.	TOTAL	AXIAL	TILT	SENSE	MAGNITUDE	PHASE	MAGNITUDE	PHASE
DEGREES	DEGREES	DB	DB	DB	RATIO	DEG.		VOLTS	DEGREES	VOLTS	DEGREES
90.00	0.00	-999.99	-999.99	-999.99	0.00000	0.00		0.00000E+00	0.00	2.60447E-14	-19.27
80.00	0.00	-999.99	5.47	5.47	0.00000	90.00	LINEAR	0.00000E+00	0.00	1.96595E+00	-12.96
70.00	0.00	-999.99	2.22	2.22	0.00000	90.00	LINEAR	0.00000E+00	0.00	1.35281E+00	25.54
60.00	0.00	-999.99	3.72	3.72	0.00000	-90.00	LINEAR	0.00000E+00	0.00	1.60829E+00	128.22
50.00	0.00	-999.99	6.29	6.29	0.00000	-90.00	LINEAR	0.00000E+00	0.00	2.16129E+00	173.13
40.00	0.00	-999.99	5.21	5.21	0.00000	-90.00	LINEAR	0.00000E+00	0.00	1.90765E+00	-138.23
30.00	0.00	-999.99	5.54	5.54	0.00000	90.00	LINEAR	0.00000E+00	0.00	1.98207E+00	-87.12
20.00	0.00	-999.99	6.64	6.64	0.00000	90.00	LINEAR	0.00000E+00	0.00	2.25072E+00	-54.45
10.00	0.00	-999.99	7.17	7.17	0.00000	90.00	LINEAR	0.00000E+00	0.00	2.39201E+00	-36.95
0.00	0.00	-999.99	7.30	7.30	0.00000	90.00	LINEAR	0.00000E+00	0.00	2.42688E+00	-31.27
-10.00	0.00	-999.99	7.17	7.17	0.00000	90.00	LINEAR	0.00000E+00	0.00	2.39201E+00	-36.95
-20.00	0.00	-999.99	6.64	6.64	0.00000	90.00	LINEAR	0.00000E+00	0.00	2.25072E+00	-54.45
-30.00	0.00	-999.99	5.54	5.54	0.00000	90.00	LINEAR	0.00000E+00	0.00	1.98207E+00	-87.12
-40.00	0.00	-999.99	5.21	5.21	0.00000	-90.00	LINEAR	0.00000E+00	0.00	1.90765E+00	-138.23
-50.00	0.00	-999.99	6.29	6.29	0.00000	-90.00	LINEAR	0.00000E+00	0.00	2.16129E+00	173.13
-60.00	0.00	-999.99	3.72	3.72	0.00000	-90.00	LINEAR	0.00000E+00	0.00	1.60829E+00	128.22
-70.00	0.00	-999.99	2.22	2.22	0.00000	90.00	LINEAR	0.00000E+00	0.00	1.35281E+00	25.54
-80.00	0.00	-999.99	5.47	5.47	0.00000	90.00	LINEAR	0.00000E+00	0.00	1.96595E+00	-12.96
-90.00	0.00	-999.99	-999.99	-999.99	0.00000	0.00		0.00000E+00	0.00	2.60447E-14	-19.27

The sample gives us a chance to see some NEC conventions as well as view a pattern report for a linearly polarized antenna. Wherever division-by-zero or division-by-infinity (or by infinitesimals) might be a problem, NEC will substitute values such as -999.99. The axial ratio is universally zero, while the tilt angle changes values according to the quantities involved in its calculation. We may ignore the value,

focusing on the sense instead. Note that the values along the horizon produce no sense, since, for this type of case, they do not yield a valid field reading.

We may compare the linearly polarized Yagi with a similar pattern report at 10° intervals for our simple 5-turn helix over perfect ground. See **Table 12**.

Table 12. 5-Turn Helix Pattern Data

- - ANGLES - -		- POWER GAINS -			- - - POLARIZATION - - -			- - - E(THETA) - - -		- - - E(PHI) - - -	
THETA	PHI	VERT.	HOR.	TOTAL	AXIAL	TILT	SENSE	MAGNITUDE	PHASE	MAGNITUDE	PHASE
DEGREES	DEGREES	DB	DB	DB	RATIO	DEG.		VOLTS	DEGREES	VOLTS	DEGREES
-90.00	90.00	-9.36	-148.77	-9.357	0.00000	0.00	LINEAR	1.03655E-01	70.66	1.10934E-08	-51.70
-80.00	90.00	-7.05	-6.59	-3.801	0.40133	-47.10	RIGHT	1.35220E-01	83.37	1.42590E-01	-52.82
-70.00	90.00	-3.56	-3.67	-0.607	0.20487	-44.61	RIGHT	2.01953E-01	99.75	1.99439E-01	-57.10
-60.00	90.00	-2.80	-6.54	-1.269	0.06595	-32.93	LEFT	2.20486E-01	116.54	1.43387E-01	-71.72
-50.00	90.00	-5.07	-10.68	-4.018	0.35876	21.30	LEFT	1.69708E-01	157.82	8.90534E-02	-151.60
-40.00	90.00	-1.02	-2.59	1.275	0.56022	35.00	RIGHT	2.70616E-01	-135.73	2.25904E-01	164.19
-30.00	90.00	4.83	1.49	6.483	0.68079	1.68	RIGHT	5.30634E-01	-112.46	3.61516E-01	158.86
-20.00	90.00	8.19	3.33	9.421	0.56596	-4.79	RIGHT	7.81870E-01	-104.15	4.46826E-01	160.14
-10.00	90.00	9.89	3.99	10.887	0.50102	-4.55	RIGHT	9.50856E-01	-100.57	4.81993E-01	162.68
0.00	90.00	10.39	3.84	11.261	0.46544	-3.89	RIGHT	1.00721E+00	-99.56	4.73544E-01	163.94
10.00	90.00	9.83	2.93	10.635	0.44749	-3.71	RIGHT	9.43675E-01	-100.68	4.26509E-01	162.74
20.00	90.00	8.05	1.20	8.865	0.45047	-3.45	RIGHT	7.69033E-01	-104.32	3.49384E-01	159.62
30.00	90.00	4.56	-1.46	5.530	0.49995	0.19	RIGHT	5.14647E-01	-112.48	2.57304E-01	157.80
40.00	90.00	-1.65	-4.82	0.060	0.50176	27.07	RIGHT	2.51829E-01	-135.28	1.74695E-01	165.86
50.00	90.00	-6.13	-6.49	-3.297	0.35333	43.47	LEFT	1.50288E-01	152.44	1.44159E-01	-168.60
60.00	90.00	-3.18	-5.19	-1.059	0.74593	-18.59	LEFT	2.11052E-01	109.98	1.67502E-01	-149.83
70.00	90.00	-3.54	-5.01	-1.201	0.56213	-35.58	LEFT	2.02554E-01	94.54	1.70983E-01	-145.53
80.00	90.00	-6.46	-8.74	-4.441	0.42198	-34.22	LEFT	1.44683E-01	81.98	1.11320E-01	-145.85
90.00	90.00	-8.48	-151.11	-8.476	0.00000	0.00	LINEAR	1.14726E-01	73.72	8.47569E-09	-146.31

The 0° line replicates the sample pattern report line with which we started. The fuller table reveals some other features of elliptical polarization in antennas. For example, the sense may shift as we sample the far field at different angles. Depending on the elevation angle, the sense shifts from left to right and back to left again. At the lowest angle, the sense is linear, although the axial ratio and tile angles are both zero. Unlike the case of the Yagi, the quantities do not include either a zero field strength or a -999.99 gain value. Hence, a value can be calculated, but turns out to be too close to zero to show any digits in the axial ratio or the tilt angle columns.

Before we go further in our exploration of what happens to the patterns of seemingly circularly polarized antennas, we should pause to wonder if it is possible to calculate left-hand and right-hand patterns in terms of circular components instead of vertical and horizontal components. The key to the calculation lies in the 4 right-most columns of information in our original sample line from the radiation pattern report (and the corresponding columns in **Table 11** and **Table 12**). These columns provide the magnitude and phase angle of Etheta and Ephi, components of the far field. If the RP command specifies a distance, then the values are in peak volts per meters. If the command does not specify a distance, then the values are in peak volts as the distance becomes indefinitely large. In either case, a linearly polarized antenna will show one of the two magnitudes as zero or very close to zero if the antenna is aligned parallel to the X-Y axes or parallel to the Z-axis. See **Table 11** for a sample where the values of Etheta are zero.

By sorting each of the values into real and imaginary components and re-combining them, we may calculate the gain (as a power ratio and in dBic or dBi-circular) of both left-handed and right-handed circular patterns. **Appendix 2** provides guidance in tracking the calculations through the various steps of one procedure that will arrive at the necessary power gain levels to create circular polarization patterns. If a given software implementation of NEC performs the calculation, it does so as a post-core-run function, converting the values derived from NEC's report into the values necessary to produce circularly polarized patterns. If a particular implementation does not provide the necessary data, one can set up a spreadsheet to obtain them. For the moment, we only need to note that we can calculate the desired patterns. Moreover, the left-hand and the right hand power ratios may be added and then converted to a value in dBic in the same way that we earlier added the power ratios of the vertical and horizontal components to arrive at the total field power gain. In fact, we can return to our circularly polarized sample antennas from earlier discussions to see the process in action.

1. *A 4-Element Circularly Polarized Quad Beam*: The first of our circularly polarized antennas was a 4-element quad beam that used a ¼-λ phasing line between corner feedpoints to create a turnstile driver and beam. For our samples, we can point the beam upward using the 7.5-λ base height that we originally used. **Table 13** provides samples from the radiation table at 10° increments, while **Fig. 21** shows the antenna outline with 2 elevation patterns. The upper pattern shows the total field and the vertical and horizontal components. The lower pattern shows the right-hand and the left-hand circular components of the total field.

Table 13. 4-Element Quad

- - - RADIATION PATTERNS - - -

- - ANGLES - -		- POWER GAINS -			- - - POLARIZATION - - -			- - - E(THETA) - - -		- - - E(PHI) - - -	
THETA DEGREES	PHI DEGREES	VERT. DB	HOR. DB	TOTAL DB	AXIAL RATIO	TILT DEG.	SENSE	MAGNITUDE VOLTS	PHASE DEGREES	MAGNITUDE VOLTS	PHASE DEGREES
90.00	0.00	-999.99	-999.99	-999.99	0.00000	0.00		2.15684E-15	25.42	7.41758E-14	35.63
80.00	0.00	-19.94	-4.48	-4.36	0.15156	-85.77	RIGHT	1.10678E-01	155.90	6.56241E-01	40.51
70.00	0.00	-14.64	-8.50	-7.56	0.40008	73.62	RIGHT	2.03571E-01	-119.82	4.12845E-01	179.78
60.00	0.00	-9.66	-6.38	-4.70	0.67678	82.97	RIGHT	3.61508E-01	-77.83	5.27339E-01	-162.28
50.00	0.00	-3.63	-1.50	0.57	0.77615	82.93	RIGHT	7.23391E-01	-55.76	9.24612E-01	-142.18
40.00	0.00	0.86	1.88	4.41	0.86923	73.29	RIGHT	1.21369E+00	-76.72	1.36397E+00	-162.29
30.00	0.00	3.96	4.18	7.08	0.94117	56.93	RIGHT	1.73424E+00	-159.55	1.77726E+00	113.62
20.00	0.00	6.09	6.01	9.06	0.93108	41.03	RIGHT	2.21595E+00	46.95	2.19426E+00	-39.00
10.00	0.00	6.76	6.53	9.66	0.93008	34.53	RIGHT	2.39200E+00	175.67	2.33093E+00	89.54
0.00	0.00	7.62	7.38	10.51	0.92647	34.37	RIGHT	2.64052E+00	-142.60	2.56851E+00	131.47
-10.00	0.00	6.73	6.61	9.68	0.92661	39.84	RIGHT	2.38499E+00	175.56	2.35271E+00	89.85
-20.00	0.00	6.01	6.26	9.15	0.92745	56.37	RIGHT	2.19509E+00	46.95	2.25981E+00	-39.07
-30.00	0.00	3.84	4.60	7.24	0.89012	69.52	RIGHT	1.70895E+00	-159.83	1.86565E+00	114.54
-40.00	0.00	0.76	2.17	4.53	0.84320	81.49	RIGHT	1.19888E+00	-76.43	1.41104E+00	-163.56
-50.00	0.00	-3.78	-1.22	0.70	0.74182	85.74	RIGHT	7.11065E-01	-55.59	9.55195E-01	-143.02
-60.00	0.00	-10.04	-5.11	-3.90	0.56296	-86.06	RIGHT	3.45849E-01	-76.24	6.10255E-01	-170.99
-70.00	0.00	-15.04	-6.33	-5.78	0.35034	83.67	RIGHT	1.94601E-01	-116.94	5.29911E-01	168.42
-80.00	0.00	-20.13	-3.82	-3.72	0.11321	-84.13	RIGHT	1.08252E-01	158.97	7.07929E-01	27.40
-90.00	0.00	-999.99	-999.99	-999.99	0.00000	0.00		2.11952E-15	28.70	7.99304E-14	23.62

Except for radiation pattern calculations for the horizon--which are too low to record as power gain levels--the tabulated values show a right-hand polarization sense for the antenna at all sampled angles. However, the axial ratio varies with the sampling elevation (theta) angle, indicating that we have elliptical polarization. As we approach the zenith angle that is also the aiming angle for the antenna, the axial ratio exceeds 0.9. Axial ratios of this magnitude indicate a very good practical approximation of true or perfect circular polarization.

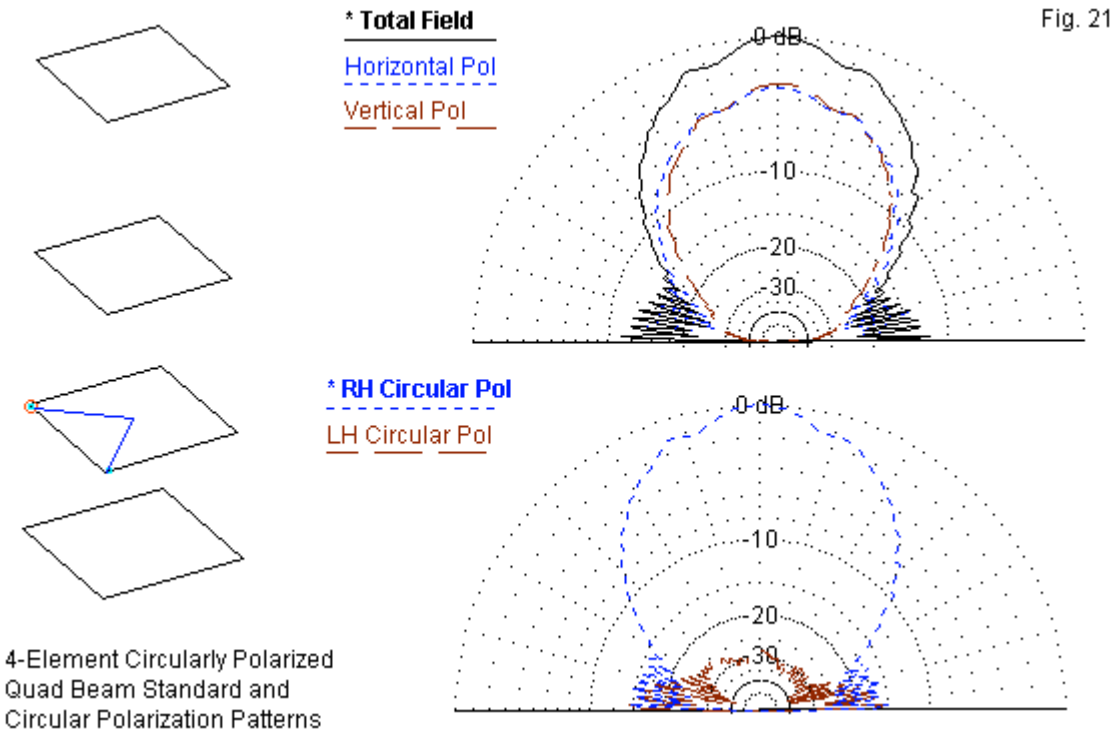

Fig. 21

4-Element Circularly Polarized Quad Beam Standard and Circular Polarization Patterns

The lower pattern in **Fig. 21** tends to confirm the observations about the pattern quality in the direction in which we have aimed the array. The feed system is for right-hand circular polarization, and that pattern far exceeds the left-hand pattern in strength in all generally upward directions.

Notice that the two sets of radiation patterns show very different information. The vertical and horizontal components of the total field have very nearly equal strength and contribute equally to the total field that is about 3 dB stronger than either component field. However, the circular field components have very different strengths. The desired component dominates by nearly 30 dB over the undesired component. The exact level of dominance in a turnstile driver system will, of course, depend upon the precision with which we can establish the driver phasing. Precision in reality is normally more difficult to attain than in models.

2. *A Circularly Polarized 8-Element Yagi with Crossed Elements*: The Yagis that we examined used separate driver elements, but with a similar 90° phasing line to achieve relatively exacting quadrature feed. The precision of the modeled antenna shows up in the truncated radiation pattern data in **Table 13**. The axial ratio overhead is again greater than 0.9, indicating a good approximation of true circular polarization. Like the pattern for the quad, the sense is right at all angles above the horizon.

Table 14. 8-Element Yagi

- - ANGLES - -		- POWER GAINS -			- - - POLARIZATION - - -			- - - E(THETA) - - -		- - - E(PHI) - - -	
								- - - RADIATION PATTERNS - - -			
THETA DEGREES	PHI DEGREES	VERT. DB	HOR. DB	TOTAL DB	AXIAL RATIO	TILT DEG.	SENSE	MAGNITUDE VOLTS	PHASE DEGREES	MAGNITUDE VOLTS	PHASE DEGREES
90.00	0.00	-999.99	-999.99	-999.99	0.00000	0.00		1.58256E-14	-5.86	9.08461E-13	-8.52
80.00	0.00	-25.34	-4.49	-4.46	0.09003	89.37	RIGHT	2.79823E+00	119.72	3.08526E+01	36.60
70.00	0.00	-15.96	-3.82	-3.56	0.23455	85.56	RIGHT	8.23736E+00	-104.54	3.33439E+01	-177.26
60.00	0.00	-18.58	-11.70	-10.89	0.43013	-81.81	RIGHT	6.09409E+00	-19.54	1.34612E+01	-124.51
50.00	0.00	-16.52	-12.41	-10.99	0.58957	-77.76	RIGHT	7.72569E+00	-116.22	1.23986E+01	140.88
40.00	0.00	-2.58	0.96	2.55	0.66505	-89.56	RIGHT	3.84374E+01	-114.46	5.77928E+01	155.18
30.00	0.00	3.52	5.79	7.81	0.76789	86.33	RIGHT	7.75669E+01	-175.03	1.00784E+02	96.92
20.00	0.00	7.08	8.55	10.88	0.84358	86.45	RIGHT	1.16914E+02	38.37	1.38408E+02	-50.42
10.00	0.00	7.68	8.50	11.12	0.90873	87.50	RIGHT	1.25219E+02	172.14	1.37745E+02	82.62
0.00	0.00	9.20	9.91	12.58	0.92060	84.88	RIGHT	1.49247E+02	-144.07	1.61906E+02	126.77
-10.00	0.00	7.68	8.50	11.12	0.90873	87.50	RIGHT	1.25219E+02	172.14	1.37745E+02	82.62
-20.00	0.00	7.08	8.55	10.88	0.84358	86.45	RIGHT	1.16914E+02	38.37	1.38408E+02	-50.42
-30.00	0.00	3.52	5.79	7.81	0.76789	86.33	RIGHT	7.75669E+01	-175.03	1.00784E+02	96.92
-40.00	0.00	-2.58	0.96	2.55	0.66506	-89.56	RIGHT	3.84374E+01	-114.46	5.77928E+01	155.18
-50.00	0.00	-16.52	-12.41	-10.99	0.58957	-77.76	RIGHT	7.72569E+00	-116.22	1.23986E+01	140.88
-60.00	0.00	-18.58	-11.70	-10.89	0.43013	-81.81	RIGHT	6.09409E+00	-19.54	1.34612E+01	-124.51
-70.00	0.00	-15.96	-3.82	-3.56	0.23455	85.56	RIGHT	8.23736E+00	-104.54	3.33439E+01	-177.26
-80.00	0.00	-25.34	-4.49	-4.46	0.09003	89.37	RIGHT	2.79823E+00	119.72	3.08526E+01	36.60
-90.00	0.00	-999.99	-999.99	-999.99	0.00000	0.00		1.58153E-14	-5.86	9.08461E-13	-8.52

Fig. 22 shows the antenna outline and the same two types of patterns that we examined for the quad. In every component, the patterns display the ripples that we saw in the total-field pattern during the earlier discussion of the antenna. These ripples appear to be endemic to virtually any antenna over ground, although the use of planar reflectors with certain types of antenna may attenuate the ripples at very high angles if the reflector surface is sufficiently large. Once more, the right-hand circular pattern dominates. In this case, the differential is at least 20 dB, with close to 30-dB differential directly overhead, where we have aimed the antenna.

Since the cross-element Yagi is aimed at its target, the poorer level of circularity to the polarization at lower elevation angles presents no problems with respect to a satellite target. However, at very low angles, the free-space pattern sidelobes do create fairly significant low-angle sidelobes when we aim the antenna directly or nearly directly upward. The maximum gain of these sidelobes is less than 15 dB down from the main upward lobe. In some locations, depending upon the surroundings, the sidelobes may be sensitive to noise and unwanted signals. Even for short Yagis, such as the 8-element version shown here, the use of designs that provide greater sidelobe attenuation or suppression may be advisable. Satellite service may profit from the use of OWA design techniques. At the prescribed boom length, an 8-element crossed-element OWA Yagi provides no gain deficit relative to more standard designs but a much lower sidelobe level.

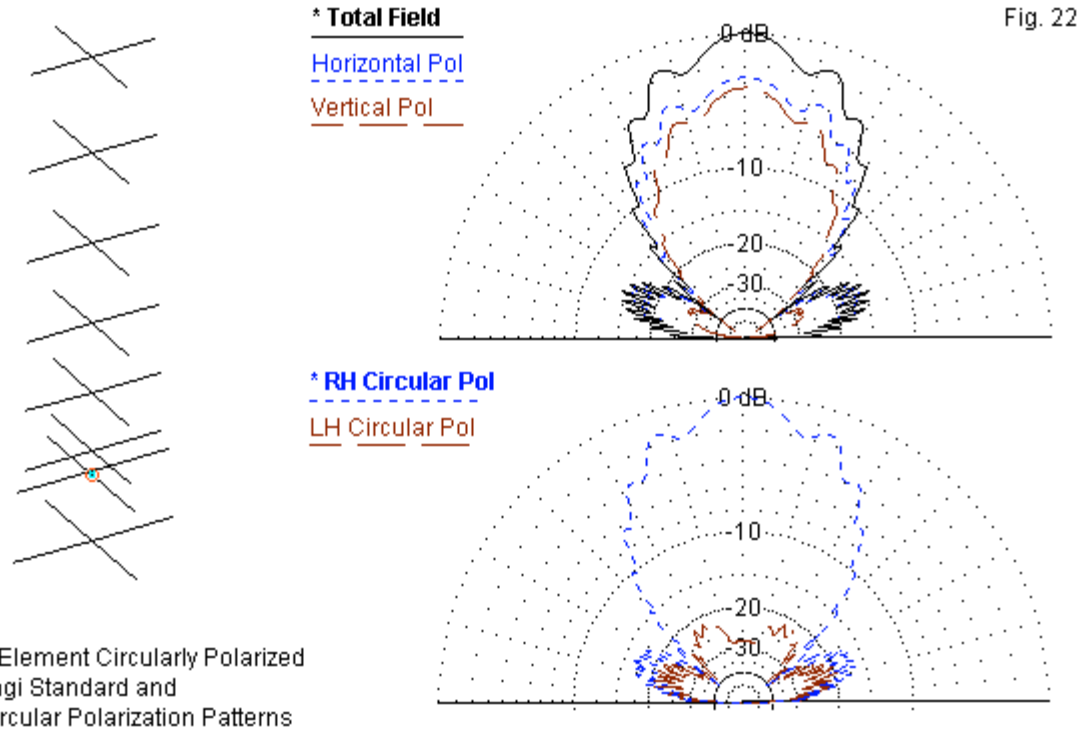

Fig. 22

8-Element Circularly Polarized
Yagi Standard and
Circular Polarization Patterns

3. *A Circularly Polarized 12-Element Yagi with Crossed Elements*: Since the 12-element Yagi is an extended version of the 8-element array, we would expect the axial ratio to be similar if we aim the beam upward and sample at 10° intervals. **Table 14** provides a partial confirmation of this expectation. Directly overhead (0° theta), the axial ratio is about 0.87, slightly lower than the values for the quad and the shorter Yagi beam. Like the other two beams, the 12-element Yagi maintains a right sense or dominant right-hand elliptical polarization for all of the elevation angles sampled in the table.

Table 15. 12-element Yagi

- - - RADIATION PATTERNS - - -

- - ANGLES - -		- POWER GAINS -			- - - POLARIZATION - - -			- - - E(THETA) - - -		- - - E(PHI) - - -	
THETA DEGREES	PHI DEGREES	VERT. DB	HOR. DB	TOTAL DB	AXIAL RATIO	TILT DEG.	SENSE	MAGNITUDE VOLTS	PHASE DEGREES	MAGNITUDE VOLTS	PHASE DEGREES
90.00	0.00	-999.99	-999.99	-999.99	0.00000	0.00		2.95192E-14	53.69	1.93205E-12	55.42
80.00	0.00	-26.08	-4.32	-4.29	0.06822	-87.43	RIGHT	2.56274E+00	137.58	3.13926E+01	14.44
70.00	0.00	-19.14	-6.58	-6.34	0.23554	89.86	RIGHT	5.70065E+00	-91.86	2.42009E+01	178.69
60.00	0.00	-14.48	-5.64	-5.11	0.35550	-86.28	RIGHT	9.73856E+00	-84.58	2.69551E+01	176.38
50.00	0.00	-10.72	-6.79	-5.32	0.63139	-85.28	RIGHT	1.50155E+01	-24.72	2.36126E+01	-119.19
40.00	0.00	-10.62	-7.25	-5.60	0.65883	-79.83	RIGHT	1.51946E+01	-113.67	2.24072E+01	147.83
30.00	0.00	1.75	3.61	5.79	0.79023	-77.71	RIGHT	6.31476E+01	167.80	7.81705E+01	72.15
20.00	0.00	7.97	9.12	11.59	0.83700	-69.26	RIGHT	1.29154E+02	26.09	1.47478E+02	-70.67
10.00	0.00	9.30	9.85	12.59	0.86312	-58.00	RIGHT	1.50516E+02	165.08	1.60493E+02	67.52
0.00	0.00	10.92	11.34	14.15	0.87372	-55.34	RIGHT	1.81544E+02	-151.36	1.90364E+02	111.42
-10.00	0.00	9.30	9.85	12.59	0.86312	-58.00	RIGHT	1.50516E+02	165.08	1.60493E+02	67.52
-20.00	0.00	7.97	9.12	11.59	0.83700	-69.26	RIGHT	1.29154E+02	26.09	1.47478E+02	-70.67
-30.00	0.00	1.75	3.61	5.79	0.79023	-77.71	RIGHT	6.31476E+01	167.80	7.81705E+01	72.15
-40.00	0.00	-10.62	-7.25	-5.60	0.65883	-79.83	RIGHT	1.51946E+01	-113.67	2.24072E+01	147.83
-50.00	0.00	-10.72	-6.79	-5.32	0.63139	-85.28	RIGHT	1.50155E+01	-24.72	2.36126E+01	-119.19
-60.00	0.00	-14.48	-5.64	-5.11	0.35550	-86.28	RIGHT	9.73857E+00	-84.58	2.69551E+01	176.38
-70.00	0.00	-19.14	-6.58	-6.34	0.23554	89.86	RIGHT	5.70065E+00	-91.86	2.42009E+01	178.69
-80.00	0.00	-26.08	-4.32	-4.29	0.06822	-87.43	RIGHT	2.56274E+00	137.58	3.13926E+01	14.44
-90.00	0.00	-999.99	-999.99	-999.99	0.00000	0.00		2.95131E-14	53.70	1.93205E-12	55.42

Like the 8-element Yagi, the 12-element array shows a fairly rapid decline in circularity as we move away from the vertical aiming angle. As well, the antenna displays its double sidelobe pattern structure. Hence, it may be equally susceptible to noise and unwanted signals. The advantage of the 12-element antenna lies in the fact that the stronger sidelobes occur at higher elevation angles.

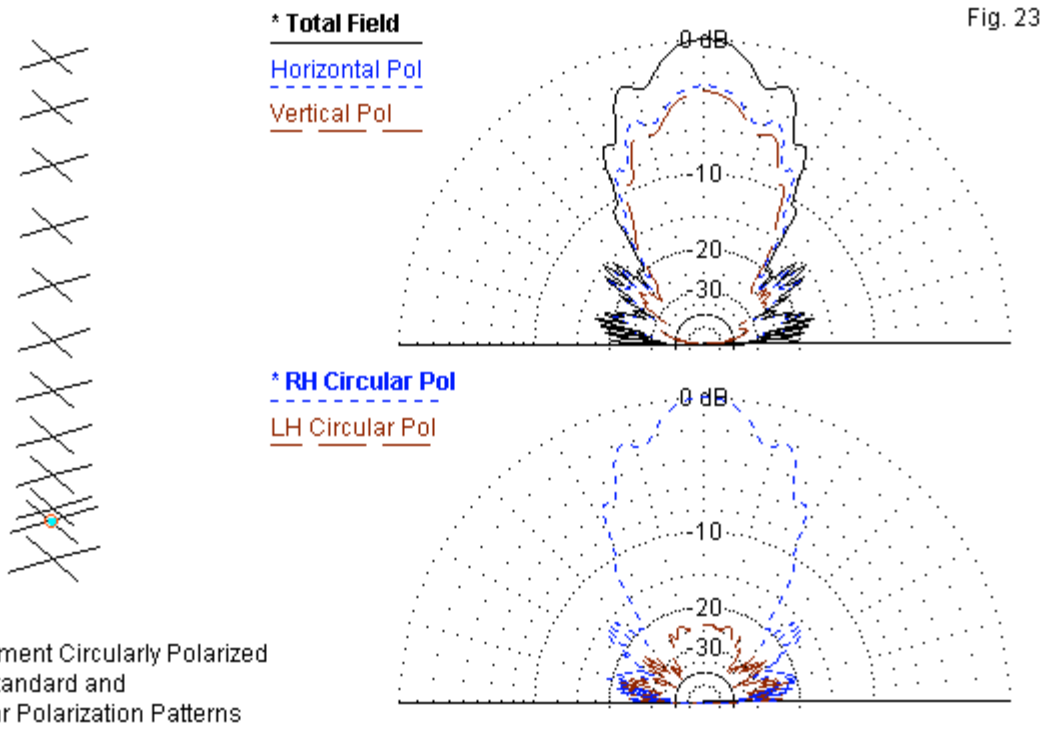

Fig. 23

Fig. 23 shows the patterns based upon vertical and horizontal components and upon left-hand and right-hand circular components. The height remains 7.5 λ at the antenna base, but the longer antenna shows increased ripple in all components as well as in the total field. The right-hand circular component shows more than 20-dB domination over the left-hand component at virtually all angles above 15° from the horizon. The three turnstiled-driver arrays establish that simple phase-line-based quadrature feed is an effective means of obtaining very nearly perfect circular polarization over a relatively narrow bandwidth. Of course, amateur satellite activities use narrow portions of the bands on which they occur. Hence, if the beamwidths and the power gain levels of any one of these antennas are satisfactory, then it is likely to serve well. In all three cases, reversing the sense of the antenna is as simple as connecting the main feedline to the other end of the phasing line.

4. *A Circularly Polarized 10-Turn Axial-Mode Antenna*: The sample axial-mode helical antenna that we discussed in the previous section now reappears for an evaluation of its circular polarization. As shown in the data from **Table 16**, it does not fare as well as the arrays with turnstile driver systems.

Table 16. 10-Turn Axial-Mode Helix

- - - RADIATION PATTERNS - - -

- - ANGLES - -		- POWER GAINS -			- - - POLARIZATION - - -			- - - E(THETA) - - -		- - - E(PHI) - - -	
THETA	PHI	VERT.	HOR.	TOTAL	AXIAL	TILT	SENSE	MAGNITUDE	PHASE	MAGNITUDE	PHASE
DEGREES	DEGREES	DB	DB	DB	RATIO	DEG.		VOLTS	DEGREES	VOLTS	DEGREES
90.00	90.00	-999.99	-999.99	-999.99	0.00000	0.00		2.97336E-14	151.67	5.94937E-14	-97.98
80.00	90.00	-17.03	-5.74	-5.43	0.02807	-74.83	LEFT	6.13331E-02	164.69	2.25045E-01	-21.66
70.00	90.00	-8.17	-6.29	-4.12	0.30794	-52.46	RIGHT	1.70222E-01	-139.68	2.11286E-01	75.47
60.00	90.00	-9.23	-2.65	-1.79	0.17590	-66.46	LEFT	1.50527E-01	-10.67	3.21295E-01	142.96
50.00	90.00	-6.26	0.89	1.66	0.43371	-86.07	RIGHT	2.11953E-01	-92.75	4.82883E-01	169.95
40.00	90.00	-0.43	0.54	3.09	0.43141	-49.67	RIGHT	4.14588E-01	-66.48	4.63633E-01	160.57
30.00	90.00	-4.42	-17.32	-4.20	0.04309	12.54	RIGHT	2.62087E-01	-58.46	5.93545E-02	-69.98
20.00	90.00	3.18	2.49	5.86	0.66421	39.11	RIGHT	6.28445E-01	-145.48	5.80532E-01	146.90
10.00	90.00	8.69	8.68	11.69	0.81200	44.94	RIGHT	1.18474E+00	4.72	1.18420E+00	-73.43
0.00	90.00	8.69	9.06	11.89	0.93617	65.25	RIGHT	1.18476E+00	55.13	1.23657E+00	-31.99
-10.00	90.00	8.96	8.85	11.92	0.81307	43.15	RIGHT	1.22330E+00	4.30	1.20730E+00	-73.95
-20.00	90.00	3.55	2.36	6.00	0.68797	33.80	RIGHT	6.55695E-01	-142.92	5.71731E-01	146.57
-30.00	90.00	-4.33	-12.94	-3.77	0.35889	5.37	RIGHT	2.64858E-01	-47.68	9.82033E-02	-124.93
-40.00	90.00	-1.48	2.54	3.99	0.48075	-66.94	RIGHT	3.67387E-01	-75.05	5.83941E-01	164.99
-50.00	90.00	-5.23	1.16	2.06	0.47543	86.32	RIGHT	2.38804E-01	-114.49	4.97996E-01	161.46
-60.00	90.00	-12.75	-2.75	-2.34	0.22430	-77.40	LEFT	1.00414E-01	1.10	3.17529E-01	133.13
-70.00	90.00	-8.92	-3.21	-2.18	0.27282	-66.00	RIGHT	1.56144E-01	-150.30	3.01228E-01	68.12
-80.00	90.00	-25.03	-5.95	-5.89	0.09437	86.65	LEFT	2.44134E-02	-141.82	2.19806E-01	-83.33
-90.00	90.00	-999.99	-999.99	-999.99	0.00000	0.00		2.84354E-14	155.72	5.14504E-14	-82.22

The limitations do not appear in the axial ratio directly overhead. That value exceeds 0.9, indicating close to perfect circular polarization. This value exceeds the circularity obtain by models placed in direct contact with a perfect ground. However, the ratio decreases very rapidly as the angle departs from the zenith. In addition, the sense undergoes rapid changes at lower elevation angles. As shown in **Fig. 24**, the main forward (upward) lobe is freer of ripples than the Yagi patterns, but the sidelobes are less than 9-dB below the level of the main lobe.

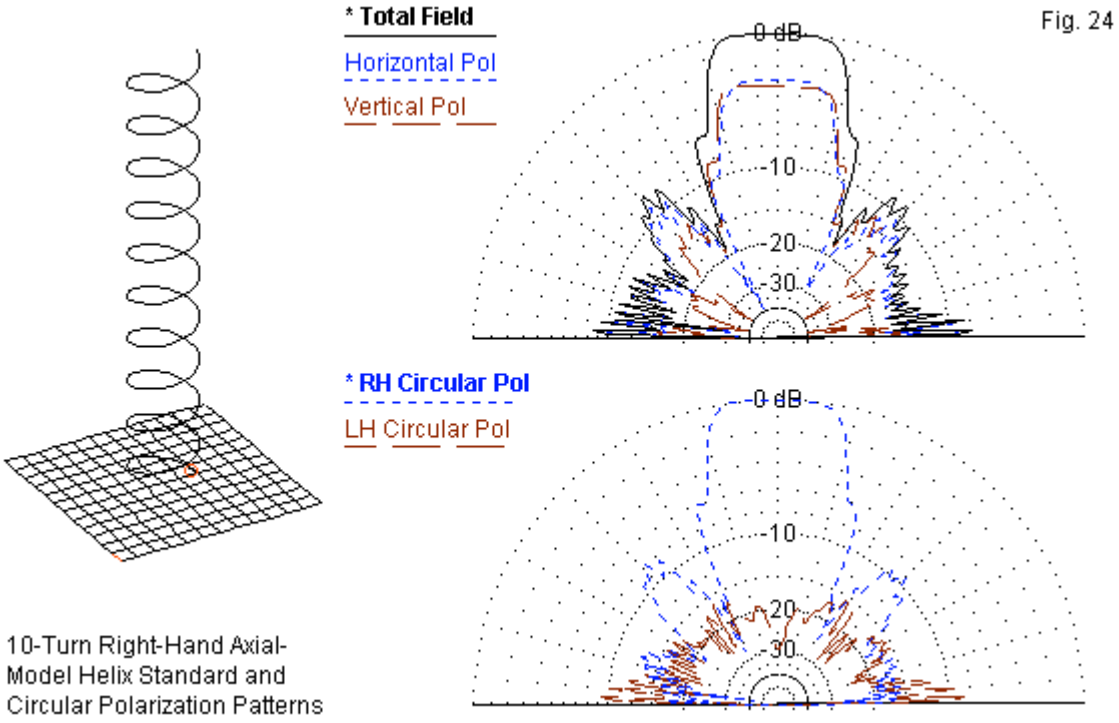

Fig. 24

10-Turn Right-Hand Axial-Model Helix Standard and Circular Polarization Patterns

With a planar reflector screen, the 10-turn axial-mode helix achieves superior performance over the earlier shorter helix connect to perfect ground, especially in terms of near-circular polarization in the direction of beam aiming. As such, it is a perfectly usable aimable and circularly polarized antenna for satellite use. However, any potential user must evaluate the importance to a given operation of the two main shortcomings. First is the existence of high-level sidelobes at both very high and very low elevation angles. Second is the need to replace the entire element if one wishes to change the polarization sense.

Fixed Antennas As Circularly Polarized

In the brief survey of the circular polarization of aimable antennas, we by-passed the small sample collection of fixed antennas with which we began our work. Before we close, we should give some attention to them, if only to answer the question: how circularly polarized are these simple arrays? The following notes will tell the story quickly enough.

1. *Turnstiled Dipoles*: The radiation pattern data (still in truncated 10° increments) for the dipole turnstile array appear in **Table 17**. Like the aimable arrays, the dipole turnstile (and all other fixed antennas in this collection) is 7.5 λ above average ground, a height that is high for 2 meters but low for 70 cm and up. Since the antenna is already set so that the broadside face is upward, we do not have to change its orientation.

The tabular data shows that the dipole turnstile maintains its right-handed circular polarization across the range of elevation angles. It even achieves a high degree of circularity at the zenith angle (0° theta). However, the patterns on **Fig. 25** show us the weaknesses of the antenna.

Table 17. Dipole Turnstile

- - - RADIATION PATTERNS - - -

- - ANGLES - - THETA DEGREES	PHI DEGREES	- POWER GAINS - VERT. DB	HOR. DB	TOTAL DB	- - - POLARIZATION - - - AXIAL RATIO	TILT DEG.	SENSE	- - - E(THETA) - - - MAGNITUDE VOLTS	PHASE DEGREES	- - - E(PHI) - - - MAGNITUDE VOLTS	PHASE DEGREES
90.00	45.00	-999.99	-999.99	-999.99	0.00000	0.00		2.14778E-13	-2.75	1.27716E-11	-3.61
80.00	45.00	-19.58	4.21	4.23	0.05761	-88.32	RIGHT	9.75569E+00	114.68	1.50886E+02	-2.21
70.00	45.00	-12.66	-3.33	-2.85	0.21472	75.08	RIGHT	2.16334E+01	-153.60	6.33213E+01	164.26
60.00	45.00	-6.14	3.96	4.37	0.31268	-89.97	RIGHT	4.58581E+01	-93.08	1.46660E+02	176.82
50.00	45.00	-3.67	2.75	3.64	0.47261	-86.06	RIGHT	6.08837E+01	-81.71	1.27547E+02	-178.14
40.00	45.00	-0.66	3.42	4.86	0.62513	89.69	RIGHT	8.61752E+01	-93.77	1.37847E+02	176.53
30.00	45.00	-8.96	-9.06	-6.00	0.96185	36.20	RIGHT	3.31303E+01	171.97	3.27431E+01	84.09
20.00	45.00	-5.64	-4.83	-2.20	0.88098	68.67	RIGHT	4.85787E+01	43.48	5.33116E+01	-41.60
10.00	45.00	-0.48	-0.41	2.56	0.99226	80.15	RIGHT	8.79699E+01	104.68	8.86161E+01	14.83
0.00	45.00	-8.14	-8.12	-5.12	0.93430	46.23	RIGHT	3.63911E+01	177.35	3.64971E+01	91.23
-10.00	45.00	-0.48	-0.41	2.56	0.99226	80.15	RIGHT	8.79699E+01	104.68	8.86161E+01	14.83
-20.00	45.00	-5.64	-4.83	-2.20	0.88098	68.67	RIGHT	4.85787E+01	43.48	5.33116E+01	-41.60
-30.00	45.00	-8.96	-9.06	-6.00	0.96185	36.20	RIGHT	3.31303E+01	171.97	3.27431E+01	84.09
-40.00	45.00	-0.66	3.42	4.86	0.62513	89.69	RIGHT	8.61752E+01	-93.77	1.37847E+02	176.53
-50.00	45.00	-3.67	2.75	3.64	0.47261	-86.06	RIGHT	6.08837E+01	-81.71	1.27547E+02	-178.14
-60.00	45.00	-6.14	3.96	4.37	0.31268	-89.97	RIGHT	4.58581E+01	-93.08	1.46660E+02	176.82
-70.00	45.00	-12.66	-3.33	-2.85	0.21472	75.08	RIGHT	2.16334E+01	-153.60	6.33213E+01	164.26
-80.00	45.00	-19.58	4.21	4.23	0.05761	-88.32	RIGHT	9.75569E+00	114.68	1.50886E+02	-2.21
-90.00	45.00	-999.99	-999.99	-999.99	0.00000	0.00		2.14807E-13	-2.74	1.27712E-11	-3.58

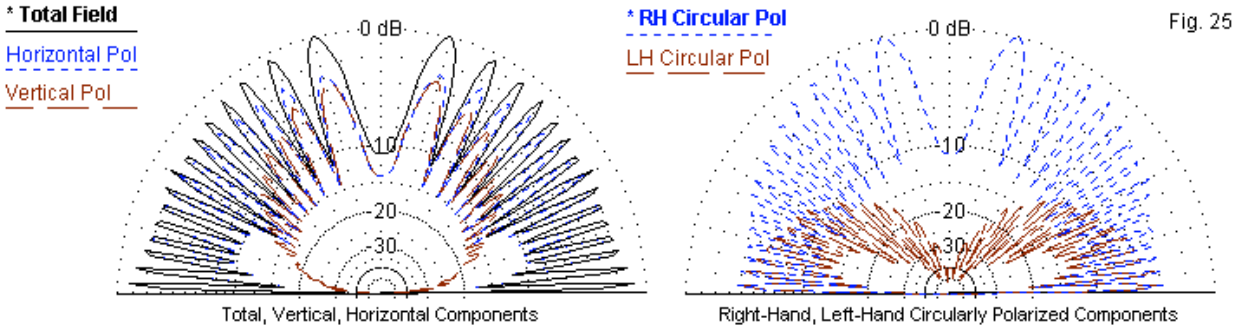

Fig. 25

Standard and Circular Elevation Patterns: Dipole Turnstile Antenna

The antenna displays maximum gain (about 5.8 dBi) at 75° and shows a strong coincidence at those high angles between the total pattern and the right-hand circularly polarized pattern. Still, the gain directly overhead is more than 10 dB below maximum gain. Had we chosen an odd increment of ¼ λ for the height, we would have obtained a dome at the zenith angle. That fact gives little solace to the other drawbacks of the antenna. The lower elevation angles show very deep nulls between lobes. Moreover, the dominance of right-hand circular polarization decreases steadily as the elevation angle decreases.

2. *Turnstiled Dipoles with a Planar Reflector Screen*: Adding a screen or planar reflector to the turnstiled dipoles converts the antenna into a directive array. **Fig. 26** shows the antenna patterns with the turnstile itself at 7.5 λ and the reflector surface ¼ λ below.

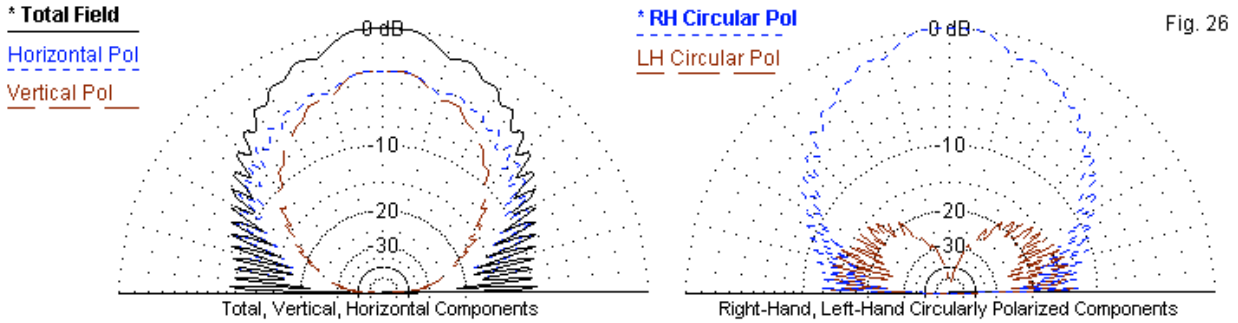

Fig. 26

Standard and Circular Elevation Patterns: Dipole Turnstile Antenna with Planar Reflector

The gain is 8.84 dBi but not quite straight up. The peak values appear 4° away from the zenith angle, although the null between peaks is completely negligible. The array maintains right-hand circular

polarization across the whole set of sampled elevation angles. As shown in **Table 18**, it achieves very good circularity at the zenith angle.

Table 18. Dipole Turnstile with Planar Reflector

- - ANGLES - -		- POWER GAINS -			- - - POLARIZATION - - -			- - - E(THETA) - - -		- - - E(PHI) - - -	
THETA	PHI	VERT.	HOR.	TOTAL	AXIAL	TILT	SENSE	MAGNITUDE	PHASE	MAGNITUDE	PHASE
DEGREES	DEGREES	DB	DB	DB	RATIO	DEG.		VOLTS	DEGREES	VOLTS	DEGREES
90.00	45.00	-999.99	-999.99	-999.99	0.00000	0.00		1.42199E-13	15.76	7.26874E-12	18.56
80.00	45.00	-21.69	-1.53	-1.49	0.09055	-87.83	RIGHT	8.07421E+00	138.67	8.22661E+01	26.17
70.00	45.00	-13.20	-2.31	-1.97	0.25765	82.98	RIGHT	2.14617E+01	-126.26	7.52031E+01	167.45
60.00	45.00	-6.80	0.77	1.47	0.41805	-89.57	RIGHT	4.48292E+01	-65.10	1.07217E+02	-155.95
50.00	45.00	-3.12	0.92	2.37	0.62708	88.49	RIGHT	6.84777E+01	-44.55	1.09119E+02	-133.09
40.00	45.00	0.37	3.18	5.01	0.72360	89.12	RIGHT	1.02401E+02	-75.26	1.41493E+02	-164.69
30.00	45.00	2.59	4.09	6.41	0.82286	76.51	RIGHT	1.32111E+02	-172.20	1.57108E+02	102.89
20.00	45.00	4.28	4.96	7.65	0.91510	75.85	RIGHT	1.60649E+02	16.42	1.73693E+02	-71.16
10.00	45.00	5.39	5.51	8.46	0.98527	79.55	RIGHT	1.82474E+02	135.90	1.85022E+02	46.20
0.00	45.00	5.82	5.82	8.83	0.99726	-49.89	RIGHT	1.91685E+02	169.93	1.91774E+02	79.77
-10.00	45.00	5.39	5.51	8.46	0.98527	79.55	RIGHT	1.82474E+02	135.90	1.85022E+02	46.20
-20.00	45.00	4.28	4.96	7.65	0.91510	75.85	RIGHT	1.60649E+02	16.42	1.73693E+02	-71.16
-30.00	45.00	2.59	4.09	6.41	0.82286	76.51	RIGHT	1.32111E+02	-172.20	1.57108E+02	102.89
-40.00	45.00	0.37	3.18	5.01	0.72360	89.12	RIGHT	1.02401E+02	-75.26	1.41493E+02	-164.69
-50.00	45.00	-3.12	0.92	2.37	0.62708	88.49	RIGHT	6.84777E+01	-44.55	1.09119E+02	-133.09
-60.00	45.00	-6.80	0.77	1.47	0.41805	-89.57	RIGHT	4.48293E+01	-65.10	1.07217E+02	-155.95
-70.00	45.00	-13.20	-2.31	-1.97	0.25765	82.98	RIGHT	2.14617E+01	-126.26	7.52031E+01	167.45
-80.00	45.00	-21.69	-1.53	-1.49	0.09055	-87.83	RIGHT	8.07422E+00	138.67	8.22661E+01	26.17
-90.00	45.00	-999.99	-999.99	-999.99	0.00000	0.00		1.42237E-13	15.77	7.27870E-12	18.66

The maximum gain of the turnstile with a planar reflector is lower than the gain of the 4-element quad. If we decide to aim this beam, we can expect the pattern to show very significant lobes and nulls near ground, even at aiming elevation angles as high as 45°. As we lower the gain of an array, we broaden the beamwidth, and even relatively high angles of aiming elevation may still show heavy interaction with the ground. As a consequence, the dipole turnstile with a planar reflector serves best at higher elevation angles as an aimable antenna. For best results at low angles, an aimable array should have enough gain so that the beamwidth is low enough not to interact seriously with the ground. This suggestion is not a plea for the use of higher gain per se. Rather, the note stresses the narrower main-lobe beamwidth that usually comes with higher gain antennas.

3. *Turnstiled Quad Loops*: The two types of turnstiled quad loops--square and diamond--yielded very similar results in terms of their total patterns. We should expect very little difference in this series of tests, as shown by **Table 19** for the square quad loops and **Table 20** for the diamond loops. The diamond loop turnstile achieves nearly perfect circularity directly overhead, although the square loops produce a very acceptable value for the axial ratio. Both antennas show domes directly overhead, but the greater vertical dimension of the diamond-loop array gives that antenna slightly greater total gain at the zenith angle. With only a slight variation in the base height of each antenna, we might reverse the gain advantage directly overhead.

Table 19. Square Dual Turnstiled Quad Loops

- - ANGLES - -		- POWER GAINS -			- - - POLARIZATION - - -			- - - E(THETA) - - -		- - - E(PHI) - - -	
THETA	PHI	VERT.	HOR.	TOTAL	AXIAL	TILT	SENSE	MAGNITUDE	PHASE	MAGNITUDE	PHASE
DEGREES	DEGREES	DB	DB	DB	RATIO	DEG.		VOLTS	DEGREES	VOLTS	DEGREES
90.00	0.00	-999.99	-999.99	-999.99	0.00000	0.00		1.55735E-12	-170.45	2.01833E-11	-93.39
80.00	0.00	-28.72	4.83	4.83	0.00625	-88.85	RIGHT	4.56806E+00	70.79	2.17458E+02	-91.89
70.00	0.00	-14.98	1.50	1.59	0.12479	85.24	RIGHT	2.22291E+01	137.60	1.48171E+02	80.72
60.00	0.00	-7.95	3.56	3.86	0.26375	-88.21	RIGHT	4.99164E+01	-173.59	1.87951E+02	90.13
50.00	0.00	-8.40	-1.61	-0.78	0.44462	-83.76	RIGHT	4.74099E+01	-157.72	1.03663E+02	101.24
40.00	0.00	-3.77	0.83	2.13	0.58711	-87.21	RIGHT	8.08275E+01	-172.07	1.37254E+02	94.82
30.00	0.00	-4.25	-1.51	0.34	0.72567	84.92	RIGHT	7.64393E+01	159.46	1.04772E+02	72.75
20.00	0.00	-1.00	0.27	2.69	0.86389	87.13	RIGHT	1.11185E+02	-10.77	1.28606E+02	-99.93
10.00	0.00	-10.85	-10.41	-7.62	0.91853	63.21	RIGHT	3.57524E+01	112.77	3.75997E+01	26.68
0.00	0.00	-1.75	-1.62	1.32	0.98361	76.01	RIGHT	1.01949E+02	164.36	1.03448E+02	74.80
-10.00	0.00	-10.85	-10.41	-7.62	0.91853	63.21	RIGHT	3.57524E+01	112.77	3.75997E+01	26.68
-20.00	0.00	-1.00	0.27	2.69	0.86389	87.13	RIGHT	1.11185E+02	-10.77	1.28606E+02	-99.93
-30.00	0.00	-4.25	-1.51	0.34	0.72567	84.92	RIGHT	7.64393E+01	159.46	1.04772E+02	72.75
-40.00	0.00	-3.77	0.83	2.13	0.58711	-87.21	RIGHT	8.08275E+01	-172.07	1.37254E+02	94.82
-50.00	0.00	-8.40	-1.61	-0.78	0.44462	-83.76	RIGHT	4.74099E+01	-157.72	1.03663E+02	101.24
-60.00	0.00	-7.95	3.56	3.86	0.26375	-88.21	RIGHT	4.99164E+01	-173.59	1.87951E+02	90.13
-70.00	0.00	-14.98	1.50	1.59	0.12479	85.24	RIGHT	2.22291E+01	137.60	1.48171E+02	80.72
-80.00	0.00	-28.72	4.83	4.83	0.00625	-88.85	RIGHT	4.56808E+00	70.79	2.17458E+02	-91.89
-90.00	0.00	-999.99	-999.99	-999.99	0.00000	0.00		1.56110E-12	-170.81	2.01833E-11	-93.39

Table 20. Diamond Dual Turnstiled Quad Loops

- - - RADIATION PATTERNS - - -

- - ANGLES - -		- POWER GAINS -			- - - POLARIZATION - - -			- - - E(THETA) - - -		- - - E(PHI) - - -	
THETA DEGREES	PHI DEGREES	VERT. DB	HOR. DB	TOTAL DB	AXIAL RATIO	TILT DEG.	SENSE	MAGNITUDE VOLTS	PHASE DEGREES	MAGNITUDE VOLTS	PHASE DEGREES
90.00	0.00	-999.99	-999.99	-999.99	0.00000	0.00		1.37296E-12	-78.75	2.03543E-11	-5.84
80.00	0.00	-29.69	4.63	4.63	0.00699	-88.97	RIGHT	4.06246E+00	154.50	2.11276E+02	-4.19
70.00	0.00	-15.54	2.58	2.64	0.10798	86.49	RIGHT	2.07112E+01	-129.63	1.66835E+02	169.56
60.00	0.00	-9.37	2.89	3.14	0.24007	-87.52	RIGHT	4.21796E+01	-81.34	1.72909E+02	179.02
50.00	0.00	-11.43	-4.73	-3.88	0.43273	-80.57	RIGHT	3.32670E+01	-55.91	7.19621E+01	-162.79
40.00	0.00	-5.99	-0.91	0.26	0.55170	-85.21	RIGHT	6.22067E+01	-77.18	1.11595E+02	-173.17
30.00	0.00	-2.20	0.68	2.48	0.71732	87.90	RIGHT	9.62431E+01	-105.23	1.34042E+02	166.20
20.00	0.00	0.05	1.36	3.76	0.86005	-89.82	RIGHT	1.24695E+02	81.79	1.44986E+02	-8.26
10.00	0.00	-5.21	-5.14	-2.16	0.98824	-63.89	RIGHT	6.80833E+01	-121.01	6.85786E+01	148.45
0.00	0.00	0.36	0.30	3.34	0.99156	-18.27	RIGHT	1.29285E+02	-101.47	1.28408E+02	168.24
-10.00	0.00	-5.21	-5.14	-2.16	0.98824	-63.89	RIGHT	6.80834E+01	-121.01	6.85786E+01	148.45
-20.00	0.00	0.05	1.36	3.76	0.86005	-89.82	RIGHT	1.24695E+02	81.79	1.44986E+02	-8.26
-30.00	0.00	-2.20	0.68	2.48	0.71732	87.90	RIGHT	9.62431E+01	-105.23	1.34042E+02	166.20
-40.00	0.00	-5.99	-0.91	0.26	0.55170	-85.21	RIGHT	6.22067E+01	-77.18	1.11595E+02	-173.17
-50.00	0.00	-11.43	-4.73	-3.88	0.43273	-80.57	RIGHT	3.32670E+01	-55.91	7.19620E+01	-162.79
-60.00	0.00	-9.37	2.89	3.14	0.24007	-87.52	RIGHT	4.21796E+01	-81.34	1.72909E+02	179.02
-70.00	0.00	-15.54	2.58	2.64	0.10798	86.49	RIGHT	2.07112E+01	-129.63	1.66835E+02	169.56
-80.00	0.00	-29.69	4.63	4.63	0.00699	-88.97	RIGHT	4.06246E+00	154.49	2.11276E+02	-4.19
-90.00	0.00	-999.99	-999.99	-999.99	0.00000	0.00		1.41392E-12	-79.62	2.03543E-11	-5.84

Fig. 27 shows the relevant patterns for the square quads, while **Fig. 28** does the same for the diamond quads. In both cases, we find the highest gain at a very low angle (2°), with very deep nulls between the lobes. As we move from directly overhead down toward the ground, both antennas show a gradual equalizing of the right-hand and the left-hand circular components. These facets of antenna performance do not mean that we cannot use such antennas successfully. A myriad of egg-beaters, potato-mashers, and other kitchen implements have given starting satellite users many successful contacts. What the users seem not to fully appreciate is how much their success is dependent upon the strength of the satellite signal rather than upon the pattern of their antennas.

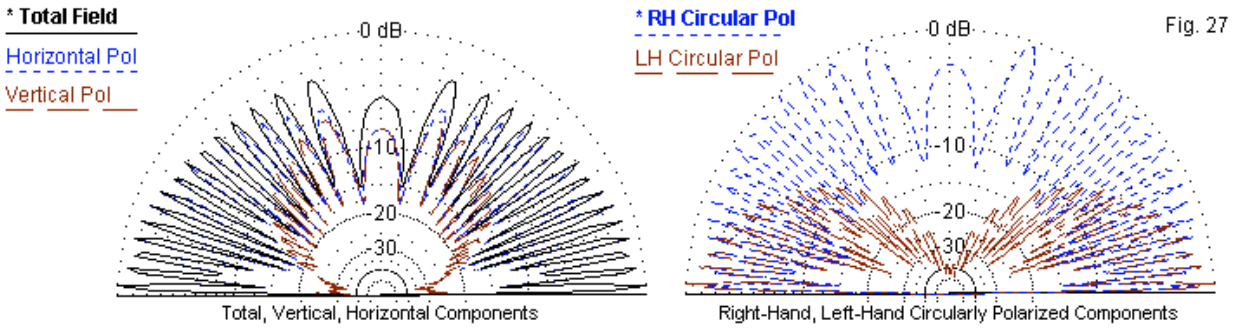

Standard and Circular Elevation Patterns: Turnstiled Square Quad Loops

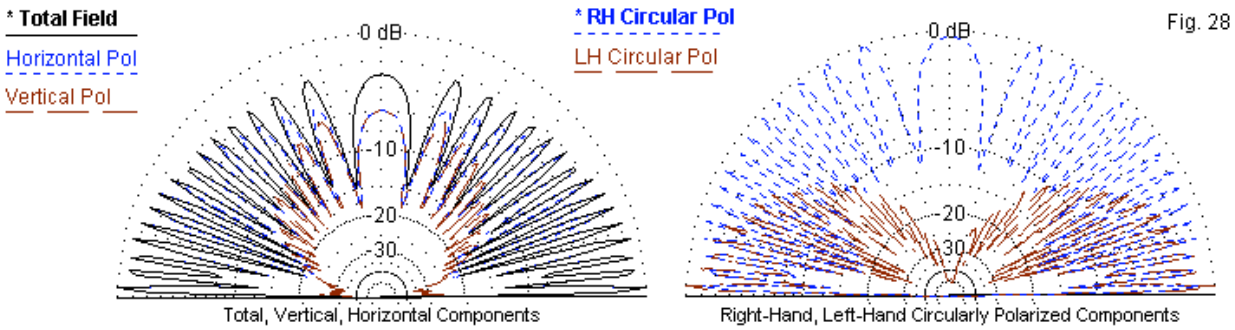

Standard and Circular Elevation Patterns: Turnstiled Diamond Quad Loops

4. *Turnstiled Moxon Rectangles*: Phase-fed Moxon rectangles showed a very good high-angle dome when we examined the total field. It remained subject to low angle lobes and nulls as we increased the antenna height. As shown in **Fig. 29** and in **Table 21**, we do not escape this phenomenon when we look at the circular polarization of the antenna. The dominant (right-hand) polarization yields reduced pattern strength at lower angles and shallower nulls between lobes. However, the overall pattern shows some

decline as we reduce the elevation angle. The nulls are not as deep as in some of the other fixed antennas, but the situation is well shy of the ideal.

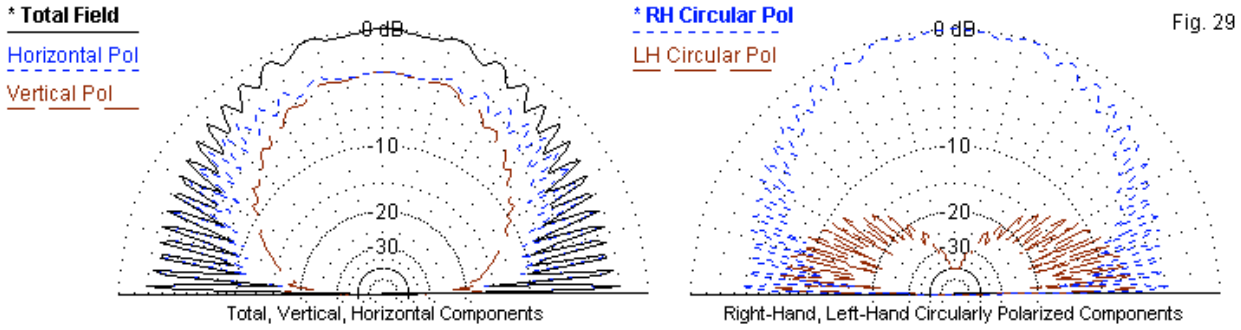

Fig. 29

Standard and Circular Elevation Patterns: Turnstiled Moxon Rectangles

Table 21. Turnstiled Moxon Rectangles

- - ANGLES - -		- POWER GAINS -			- - - POLARIZATION - - -			- - - E(THETA) - - -		- - - E(PHI) - - -	
THETA DEGREES	PHI DEGREES	VERT. DB	HOR. DB	TOTAL DB	AXIAL RATIO	TILT DEG.	SENSE	MAGNITUDE VOLTS	PHASE DEGREES	MAGNITUDE VOLTS	PHASE DEGREES
90.00	0.00	-999.99	-999.99	-999.99	0.00000	0.00		1.92748E-12	135.91	9.89238E-12	58.31
80.00	0.00	-10.94	2.86	3.03	0.19748	-87.00	RIGHT	2.32083E+01	168.68	1.13593E+02	64.40
70.00	0.00	-7.40	-0.72	0.13	0.38920	75.66	RIGHT	3.48864E+01	-89.45	7.52873E+01	-151.83
60.00	0.00	-4.20	2.96	3.73	0.43645	-87.67	RIGHT	5.04075E+01	-19.34	1.15015E+02	-113.65
50.00	0.00	-2.14	1.78	3.26	0.62385	-82.01	RIGHT	6.39412E+01	8.61	1.00377E+02	-89.06
40.00	0.00	-0.04	2.80	4.62	0.71855	-86.32	RIGHT	8.13749E+01	-14.25	1.12919E+02	-106.72
30.00	0.00	0.88	1.97	4.47	0.88080	86.75	RIGHT	9.04710E+01	-97.60	1.02629E+02	173.23
20.00	0.00	2.12	2.69	5.43	0.93620	-89.25	RIGHT	1.04377E+02	103.25	1.11488E+02	13.16
10.00	0.00	2.38	2.51	5.46	0.97535	-62.52	RIGHT	1.07569E+02	-135.61	1.09121E+02	133.22
0.00	0.00	2.79	2.78	5.80	0.98118	-43.49	RIGHT	1.12755E+02	-92.53	1.12642E+02	176.38
-10.00	0.00	2.38	2.51	5.46	0.97535	-62.52	RIGHT	1.07569E+02	-135.61	1.09121E+02	133.22
-20.00	0.00	2.12	2.69	5.43	0.93620	-89.25	RIGHT	1.04377E+02	103.25	1.11488E+02	13.16
-30.00	0.00	0.88	1.97	4.47	0.88080	86.75	RIGHT	9.04710E+01	-97.60	1.02629E+02	173.23
-40.00	0.00	-0.04	2.80	4.62	0.71855	-86.32	RIGHT	8.13750E+01	-14.25	1.12919E+02	-106.72
-50.00	0.00	-2.14	1.78	3.26	0.62385	-82.01	RIGHT	6.39413E+01	8.61	1.00377E+02	-89.06
-60.00	0.00	-4.20	2.96	3.73	0.43645	-87.67	RIGHT	5.04075E+01	-19.34	1.15015E+02	-113.65
-70.00	0.00	-7.40	-0.72	0.13	0.38920	75.66	RIGHT	3.48864E+01	-89.45	7.52873E+01	-151.83
-80.00	0.00	-10.94	2.86	3.03	0.19748	-87.00	RIGHT	2.32082E+01	168.68	1.13593E+02	64.40
-90.00	0.00	-999.99	-999.99	-999.99	0.00000	0.00		1.92657E-12	135.93	9.89238E-12	58.31

One temptation that we should note involves the relative smoothness of the Moxon pair's high-angle dome. The idea occurs almost naturally: why not simple tilt the dome to the desired elevation angle for maximum evenness of pattern at the highly used lower elevation angles? **Fig. 30** provides part of the answer.

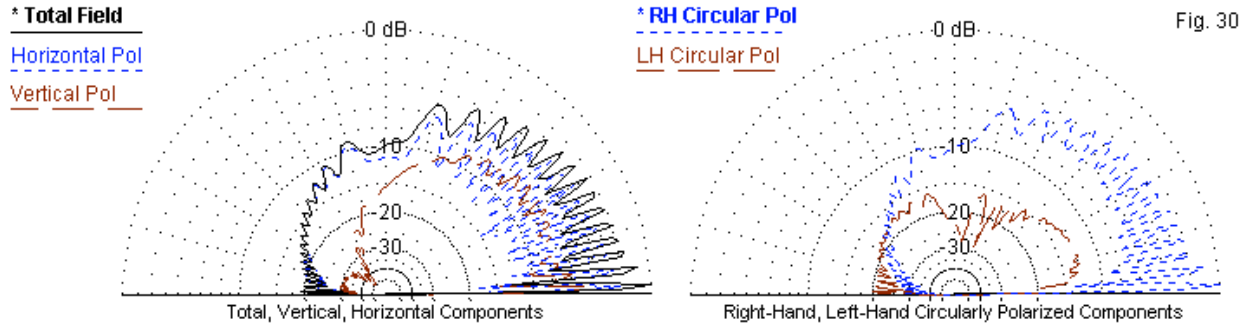

Fig. 30

Standard and Circular Elevation Patterns: Turnstiled Moxon Rectangles: Elevation Angle 30 Degrees

The Moxon remains at 7.5 λ above average ground, but now has an aiming elevation angle of 30°. Maximum gain climbs to over 10 dBi, but only at 2° above the horizon. The very-wide beamwidth of the Moxon rectangle allows heavy interaction with the ground, resulting in very large low-angle lobes and very deep nulls. However, the designed right-hand polarization remains dominant. Hence, if the satellite signal strength (minus any ground-clutter losses) is high enough, a tilted Moxon pair can serve well

enough, whether the antenna is fixed or movable in elevation. Aiming angles below 30° should not be necessary for general work with satellites for which low-angle use is standard.

5. *The Modified Lindenblad*: The last fixed antenna in our small survey is the modified Lindenblad array of 4 angled dipoles using progressive quadrature feed. If we move the feedpoints (or dipole centers) to 7.5 λ above ground, we obtain the patterns in **Fig. 31**.

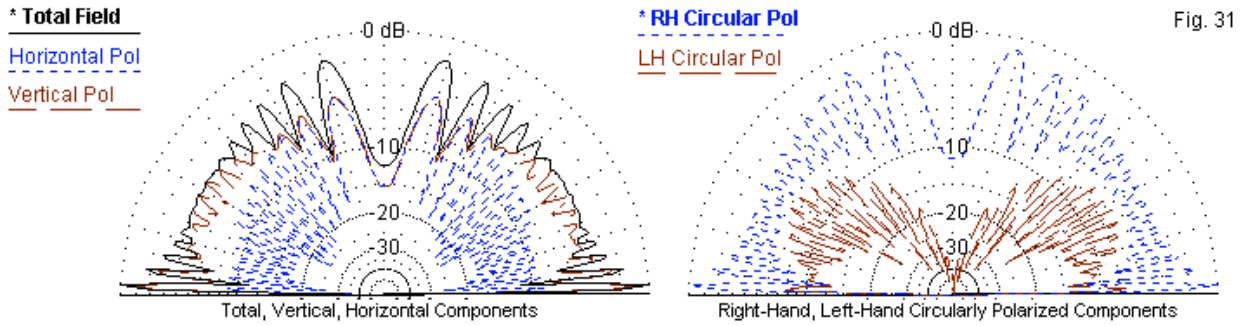

Fig. 31

Standard and Circular Elevation Patterns: Lindenblad Array

The total field for the modified Lindenblad shows quite smooth response from about 10° up to about 45°. Since the array was not designed for vertical service, it tends to show a zenith-angle null that is deeper than the others that we have seen. As the data in **Table 22** show, polarization at the zenith angle is perfectly circular, but at a very low strength.

Table 22. Lindenblad Array

- - ANGLES - -		- POWER GAINS -			- - - POLARIZATION - - -			- - - E(THETA) - - -		- - - E(PHI) - - -	
								- - - RADIATION PATTERNS - - -			
THETA DEGREES	PHI DEGREES	VERT. DB	HOR. DB	TOTAL DB	AXIAL RATIO	TILT DEG.	SENSE	MAGNITUDE VOLTS	PHASE DEGREES	MAGNITUDE VOLTS	PHASE DEGREES
90.00	45.00	-999.99	-999.99	-999.99	0.00000	0.00		2.16836E-11	-143.19	7.63158E-12	132.28
80.00	45.00	2.35	-3.03	3.45	0.51270	-9.73	RIGHT	1.72183E+02	-124.60	9.27236E+01	131.94
70.00	45.00	1.78	-10.15	2.05	0.08703	13.38	RIGHT	1.61360E+02	-28.18	4.08640E+01	-49.46
60.00	45.00	-0.21	-1.58	2.17	0.85412	-0.19	RIGHT	1.28257E+02	42.00	1.09547E+02	-48.06
50.00	45.00	0.34	-1.65	2.47	0.56686	-31.98	RIGHT	1.36671E+02	72.82	1.08646E+02	-45.46
40.00	45.00	0.42	0.12	3.28	0.95760	18.28	RIGHT	1.37925E+02	40.18	1.33208E+02	-48.34
30.00	45.00	-1.81	-12.85	-1.48	0.27933	-1.43	RIGHT	1.06758E+02	-50.39	2.99389E+01	-145.10
20.00	45.00	-3.60	-6.89	-1.93	0.59712	20.19	RIGHT	8.68289E+01	164.62	5.94738E+01	93.86
10.00	45.00	-1.19	-1.41	1.71	0.93464	-34.34	RIGHT	1.14577E+02	-117.05	1.11800E+02	149.34
0.00	45.00	-9.01	-9.01	-6.00	1.00000	42.35	RIGHT	4.65740E+01	-47.23	4.65740E+01	-137.23
-10.00	45.00	-1.19	-1.41	1.71	0.93464	-34.34	RIGHT	1.14577E+02	-117.05	1.11800E+02	149.34
-20.00	45.00	-3.60	-6.89	-1.93	0.59712	20.19	RIGHT	8.68289E+01	164.62	5.94738E+01	93.86
-30.00	45.00	-1.81	-12.85	-1.48	0.27933	-1.43	RIGHT	1.06758E+02	-50.39	2.99389E+01	-145.10
-40.00	45.00	0.42	0.12	3.28	0.95760	18.28	RIGHT	1.37925E+02	40.18	1.33208E+02	-48.34
-50.00	45.00	0.34	-1.65	2.47	0.56686	-31.98	RIGHT	1.36671E+02	72.82	1.08646E+02	-45.46
-60.00	45.00	-0.21	-1.58	2.17	0.85412	-0.19	RIGHT	1.28257E+02	42.00	1.09547E+02	-48.06
-70.00	45.00	1.78	-10.15	2.05	0.08703	13.38	RIGHT	1.61360E+02	-28.18	4.08640E+01	-49.46
-80.00	45.00	2.35	-3.03	3.45	0.51270	-9.73	RIGHT	1.72183E+02	-124.60	9.27236E+01	131.94
-90.00	45.00	-999.99	-999.99	-999.99	0.00000	0.00		2.16336E-11	-143.36	7.62842E-12	132.19

The circular polarization patterns show a feature of the array that we could not guess from looking at the total-field pattern. At all elevation angles, right-hand circular polarization shows lobes and nulls of moderate proportions. The total field pattern (which would be the same whether the components are the circular polarization patterns or the vertical and horizontal patterns) has a lower-angle smoothness that results from the combination of the circularly polarized components. For this antenna, when right-hand polarization shows a null, left-hand polarization fills in the total field with a lobe. Nevertheless, the modified Lindenblad remains a prime candidate as a fixed antenna for low-angle satellite communications.

One consequence of our examination of the circular polarization situation for the fixed antennas in our collection of samples is perhaps a revised understanding of the seeming importance of circular polarization. Even high-gain aimable antennas are subject to ripples in their patterns and off-axis degradation of circular polarization. If we wish to aim antennas at low angles, then we need to think in terms of narrow beamwidth (and consequential higher gain) as a key to maintaining pattern purity. For fixed antennas, we tend to be dependent upon the satellite signal level as a key to effective

communications. It is likely that even tilted verticals will work well if we can overcome a major hindrance to satellite signal levels: ground clutter. In times past, antenna builders would clear many acres of land in order to give their HF rhombics a clear path to their destination. We do not have that luxury today, especially since ground clutter is composed less of trees and more of high-rise buildings. Moving the entire satellite community to the tier of states from Texas up to North Dakota is equally impractical.

Conclusion

These notes have tried to develop some basic ideas too often overlooked in the search for a perfect DX and off-world antenna. Fixed antennas tend to falter either at low elevation angles or at high sky angles. Aimable antennas have interesting properties at various elevation angles, especially if the gain does not exceed certain levels. What we call circular polarization tends to be elliptical polarization carried to near circularity in some antenna designs, but only over limited portions of the antenna pattern. These summary statements are perhaps less important than the background material used to develop them, since understanding the role of antenna height, elevation angle, and methods of obtaining a desired type of performance apply far beyond the small range of sample antennas explored here.

The more we understand about antenna behavior, the more satisfying will be our operating, our building, and even our buying.

Appendix 1: The Original Lindenblad Circularly Polarized Dipole Array

The modified Lindenblad dipole array is one possibility for a fixed-position satellite antenna especially suited to capturing satellites at lower elevation angles relative to the horizon. Its origins lie in the pioneering work of N. E. Lindenblad, who first proposed the antenna design almost off-hand in a broad article on television transmitting antennas. (See N. E. Lindenblad, " Antennas and Transmission Lines at the Empire State Television Station," *Communications*, vol. 21, April, 1941, pp. 10-14 and 24-26.) After World War II, Brown and Woodward (who made numerous contributions to VHF and UHF antenna design) developed the idea in detail from Lindenblad's patent papers. (See G. H. Brown and O. M. Woodward, "Circularly Polarized Omnidirectional Antenna," *RCA Review*, vol. 8, June, 1947, pp. 259-269.) They envisioned possible aviation uses for the antenna. The overall goal for the antenna was omni-directional coverage in the X-Y plane (parallel to ground) with circular polarization. They did not design the antenna for overhead coverage.

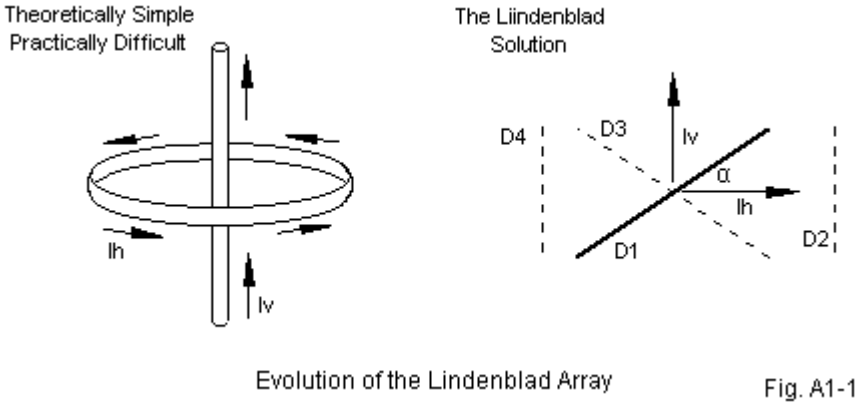

Evolution of the Lindenblad Array Fig. A1-1

Fig. A1-1 shows on the left the fundamental principle behind the Lindenblad dipole array. To achieve circular polarization, we need vertically and horizontally polarized components--shown as currents in the wires--such that they result in exactly equal fields at any distance from the antenna in any direction. The sketch shows right-hand circular polarization. The conceptual diagram is almost impossible to realize as a physical antenna. Lindenblad reasoned that an array of tilted dipole, fed in phase, would approximate the ideal situation. The right side of **Fig. A1-1** shows the solution, highlighting 1 of the 4 dipoles. If we select the proper angle for the dipole relative to the horizontal (α), then the vertical and horizontal components will be equal. The design is subject to limitations, since we have facing dipoles. The tilt angle, α, depends in part on the distance between facing dipoles. In terms better suited to calculation, the required tilt angle depends upon the radius of the circle connecting the feedpoint positions of the dipoles. Since the fields between adjacent dipoles overlap, the required tilt angle for the dipole also depends on whether we measure fields tangential to the dipole faces or at angles that bisect two dipoles. The following table shows a few of the Brown-Woodward tilt-angle calculations.

Table A1-1. Calculated Tilt Angles for Dipoles in a Lindenblad Dipole Array

Radius	Tilt Angle Relative to the Horizontal	
In λ	Facing Dipole	Between Dipoles
0.0833	15°	15° 22'
0.166	30°	32° 55'
0.25	45°	55°

The modified Lindenblad array using progressive quadrature feed uses a radius of 0.25λ. Therefore, we may simply change the phase angles of the individual feedpoints to put them all at the same phase angle. However, this seemingly simple change results in a need to change the length of the dipoles to restore resonance to each dipole. As well, we need to re-angle the dipoles in the opposite direction from those in the modified version to achieve right-hand circular polarization. **Fig. A1-2** shows what we get.

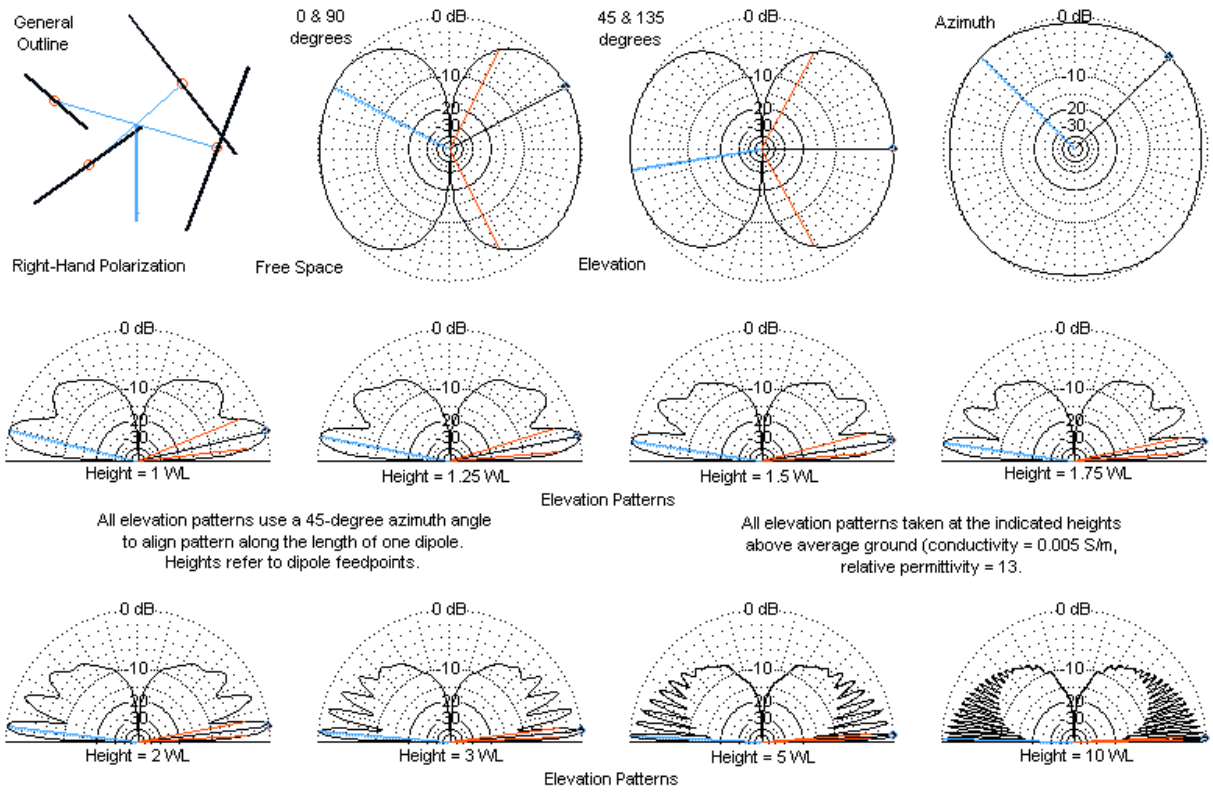

Sample Total-Field Patterns of a Right-Hand Polarized Original Lindenblad Array

Fig. A1-2

In its original configuration, the free-space elevation or theta patterns for the Lindenblad array are quite symmetrical. The slight variation in the patterns facing a dipole and the patterns at 45° to any dipole reflects the requirement for optimizing the tilt angle. In these patterns, the tilt angle is constant at 45°. The phi or azimuth pattern shows a slight squaring, comparable to the pattern of an ordinary turnstile pair of dipoles.

Over ground, we obtain elevation patterns that reflect the original uses planned for the antenna. As shown in **Fig. A1-2** and in **Table A1-2**, the strongest lobe is always the lowest lobe. As well, beamwidth of the strongest lobe is always quite narrow. The array produces a very deep null directly overhead.

Table A1-2. Critical Performance Data for an Original Lindenblad Array at Various Heights above Average Ground

Height (λ)	Gain (dBi)	Elevation Angle Of Peak Gain	Beamwidth (degrees)
1	5.28	13	16
1.25	5.51	11	12
1.5	5.72	9	10
1.75	5.83	8	9
2	5.96	7	7
3	6.18	5	5
5	6.45	3	3
10	6.73	1.5	1.5

As a consequence of these pattern features, the original Lindenblad array is not especially suitable for satellite work, although it may serve as an omni-directional antenna for point-to-point communications. Unless the target stations are using the same polarization, results are likely to be little better than with a

simple dipole turnstile. If the target station is using a comparable antenna, but with left-hand circular polarization, then the two antennas may be blind to each other.

Nevertheless, the Lindenblad array achieves a close approximation to circular polarization relative to point-to-point targets in the X-Y plane, that is, parallel to the earth's surface. At angle facing the dipoles (0°, 90°, and 180°), the axial ratio is close to 0.9. Between dipoles (at 45° and 135°) the ratio drops below 0.7, again suggesting the need to change the tilt angle for more nearly circular polarization. I all cases, the sense of polarization is right-handed.

Lindenmblad Radiation Pattern Reports in Free-Space for Phi Angles 0 to 180°

- - - RADIATION PATTERNS - - -

- - ANGLES - -		- POWER GAINS -			- - - POLARIZATION - - -			- - - E(THETA) - - -		- - - E(PHI) - - -	
THETA DEGREES	PHI DEGREES	VERT. DB	HOR. DB	TOTAL DB	AXIAL RATIO	TILT DEG.	SENSE	MAGNITUDE VOLTS	PHASE DEGREES	MAGNITUDE VOLTS	PHASE DEGREES
90.00	0.00	-3.37	-2.33	0.19	0.88674	-88.70	RIGHT	1.07851E+02	85.59	1.21611E+02	-4.72
90.00	10.00	-3.43	-2.13	0.28	0.86140	-89.08	RIGHT	1.07138E+02	85.57	1.24368E+02	-4.70
90.00	20.00	-3.58	-1.66	0.50	0.80191	-89.60	RIGHT	1.05333E+02	85.53	1.31350E+02	-4.65
90.00	30.00	-3.75	-1.15	0.75	0.74144	-89.88	RIGHT	1.03279E+02	85.47	1.39295E+02	-4.60
90.00	40.00	-3.86	-0.83	0.92	0.70553	-89.99	RIGHT	1.01937E+02	85.44	1.44483E+02	-4.57
90.00	50.00	-3.86	-0.83	0.92	0.70553	-89.99	RIGHT	1.01937E+02	85.44	1.44483E+02	-4.57
90.00	60.00	-3.75	-1.15	0.75	0.74144	-89.88	RIGHT	1.03279E+02	85.47	1.39295E+02	-4.60
90.00	70.00	-3.58	-1.66	0.50	0.80191	-89.60	RIGHT	1.05333E+02	85.53	1.31350E+02	-4.65
90.00	80.00	-3.43	-2.13	0.28	0.86140	-89.08	RIGHT	1.07138E+02	85.57	1.24368E+02	-4.70
90.00	90.00	-3.37	-2.33	0.19	0.88674	-88.70	RIGHT	1.07851E+02	85.59	1.21611E+02	-4.72
90.00	100.00	-3.43	-2.13	0.28	0.86140	-89.08	RIGHT	1.07138E+02	85.57	1.24368E+02	-4.70
90.00	110.00	-3.58	-1.66	0.50	0.80191	-89.60	RIGHT	1.05333E+02	85.53	1.31350E+02	-4.65
90.00	120.00	-3.75	-1.15	0.75	0.74144	-89.88	RIGHT	1.03279E+02	85.47	1.39295E+02	-4.60
90.00	130.00	-3.86	-0.83	0.92	0.70553	-89.99	RIGHT	1.01937E+02	85.44	1.44483E+02	-4.57
90.00	140.00	-3.86	-0.83	0.92	0.70553	-89.99	RIGHT	1.01937E+02	85.44	1.44483E+02	-4.57
90.00	150.00	-3.75	-1.15	0.75	0.74144	-89.88	RIGHT	1.03279E+02	85.47	1.39295E+02	-4.60
90.00	160.00	-3.58	-1.66	0.50	0.80191	-89.60	RIGHT	1.05333E+02	85.53	1.31350E+02	-4.65
90.00	170.00	-3.43	-2.13	0.28	0.86140	-89.08	RIGHT	1.07138E+02	85.57	1.24368E+02	-4.70
90.00	180.00	-3.37	-2.33	0.19	0.88674	-88.70	RIGHT	1.07851E+02	85.59	1.21611E+02	-4.72
90.00	190.00	-3.43	-2.13	0.28	0.86140	-89.08	RIGHT	1.07138E+02	85.57	1.24368E+02	-4.70

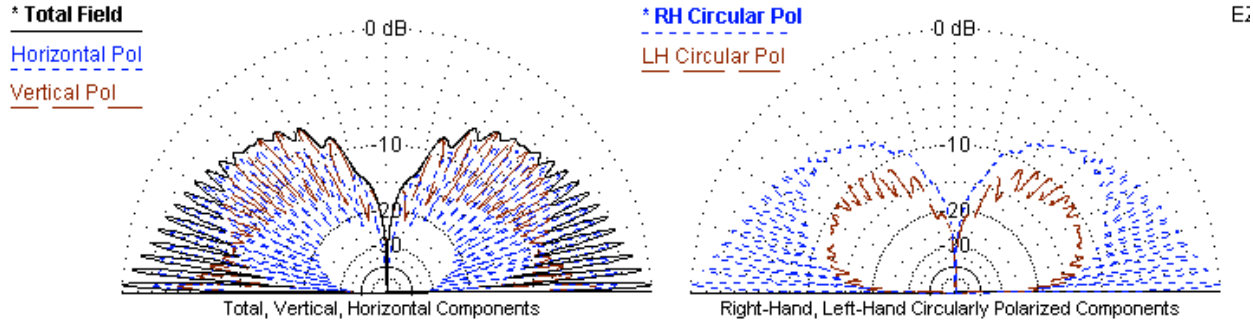

Standard and Circular Elevation Patterns: Right-Hand Polarized Original Lindenblad Array

Fig. A1-3

Fig. A1-3 shows the elevation patterns for the original Lindenblad at a height of 7.5 λ above average ground. Although the right-hand circular polarization component dominates the pattern at the right, the multiplicity of lobes and nulls tends to disqualify the original array from satellite service. Compare these patterns to corresponding patterns for the modified Lindenblad with progressive quadrature feed. Although the modified version of the antenna has slightly less gain, the evenness of its pattern suggests more satisfactory satellite service at lower elevation angles.

The exploration of original Lindenblad literature is not either idle or merely historical. Some antenna builders have tried closer dipole spacing than the value recommended in the main text. To obtain satisfactory patterns, they may wish to attend to the calculations of the more nearly correct tilt angle for these closer spacings. We may yet learn much more about the modified Lindenblad array.

Appendix 2: Calculating Circular Power Gains from Field-Strength Voltages

If we model an antenna using either NEC-2 or NEC-4, then we can obtain a tabular report of the radiation pattern. Most modelers ignore the tabular data and look only at the graphical portrayal of the data, that is, at the patterns and plots. However, the tabular data includes many useful items that do not appear in the plots. The following line is just one of 180 lines of a theta (elevation) plot table.

```
                        - - - RADIATION PATTERNS - - -

  - - ANGLES - -           - POWER GAINS -       - - - POLARIZATION - - -
THETA     PHI          VERT.    HOR.      TOTAL      AXIAL      TILT    SENSE
DEGREES   DEGREES       DB       DB        DB        RATIO      DEG.
 0.00     90.00        10.39     3.84    11.261     0.46544     -3.89   RIGHT
           - - - E(THETA) - - -        - - - E(PHI) - - -
          MAGNITUDE       PHASE       MAGNITUDE      PHASE
            VOLTS         DEGREES       VOLTS        DEGREES
          1.00721E+00    -99.56       4.73544E-01    163.94
```

The data that we normally use (or see in a plot) includes the angles (translated into elevation and azimuth equivalents), plus the total power gain and sometimes the vertical and horizontal components of the total gain. We ignore the rest, although much of it is critical to understanding how we arrive at circular polarization (left-hand and right-hand) patterns and values. **Fig. A2-1** shows the model that produced the sample line, along with right-hand and left-hand circular patterns for the upright model.

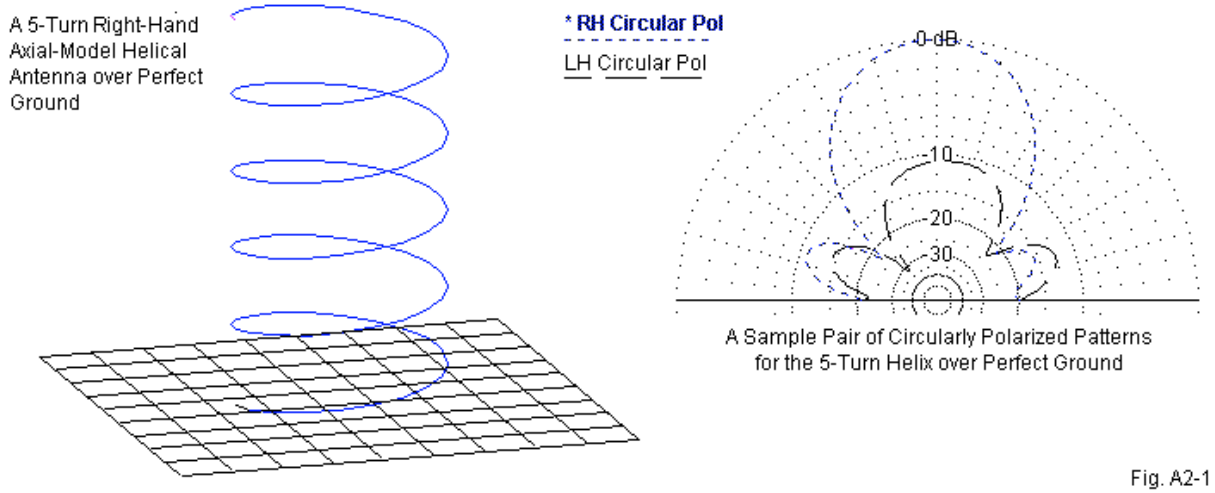

Fig. A2-1

We can calculate the pattern values for both the left-hand and right-hand patterns using the previously ignored Etheta and Ephi data. Some implementations of NEC, such as EZNEC, GNEC, NEC-Win Pro, and NEC-Win Plus, already perform these calculations. However, it is useful to understand the calculation of these values, which is a post-core-run process. In order to see how the calculation might proceed, let's repeat the relevant parts of our sample line.

```
  - - ANGLES - -   - POWER GAIN -  POLARIZATION
  THETA     PHI        TOTAL         SENSE
 DEGREES   DEGREES       DB
    0.00    90.00     11.261         RIGHT
                          - - - E(THETA) - - -       - - - E(PHI) - - -
                         MAGNITUDE     PHASE       MAGNITUDE     PHASE
                         VOLTS         DEGREES     VOLTS         DEGREES
                         1.00721E+00   -99.56      4.73544E-01   163.94
```

The procedure begins by taking the real and imaginary components of each value of E (theta and phi). They appear in terms of magnitude and phase angle in the sample line. The steps use spreadsheet notation, since that is the most likely medium for using the equations. However, you may easily translate them into standard algebraic notation.

vetr = EthetaMag * cos(Ethetaphase); theta real
veti = EthetaMag * sin(Ethetaphase); theta imaginary
vepr = EphiMag * cos(Ephiphase); phi real
vepi = EphiMag * sin(Ephiphase); phi imaginary

These initial values are simply intermediate steps. We next must re-combine the collection into units that reflect the polarization of the antenna.

velr = 0.5*(vetr + vepi); left real circular component
veli = 0.5*(veti - vepr); left imaginary circular component
verr = 0.5*(vetr - vepi); right real circular component
veri = 0.5*(veti + vepr); right imaginary circular component

Now we can combine the circular components into values of magnitude by standard "square root of squares" techniques.

elm = sqrt(velr*velr + veli*veli); left magnitude
erm = sqrt(verr*verr + veri*veri); right magnitude

We now have the magnitudes of the left-hand and the right-hand electrical fields in volts (peak)/meter. The move from these voltage magnitudes to pattern data in dBic (dBi circular) requires a few more steps. The following are the calculations required for the conversion.

a. Convert the Total Field Gain into a dimensionless gain measure.

PwrGn = antilog (base 10) (TtlFldGn/10)

b. Square the ratio of the right voltage magnitude (erm) to the left voltage magnitude (elm). This squared ratio is the ratio of the dimensionless power gains for right and left patterns.

RatSq = (erm/elm)^2

The next steps are predicated on the assumption that the sum of the two dimensionless circular power gains is the dimensionless total field power gain.

c. Right Gain and Left Gain are 2 unknowns that are subject to simultaneous equations. Selecting Right Gain first, we obtain the following 2 steps.

GnRt = RatSq * PwrGn/(1 + RatSq)

GnRtdBi = 10 * log(GnRt)

d. Left Gain is simply the power gain minus the right gain (all dimensionless).

GnLf = PwrGn - GnRt

GnLfdBi = 10 * log(GnLf)

For our single sample line of RP 0 reporting, we obtain the following values.

```
Theta      ERM      ELM      Sense    RatSq    PwrGn
0          .7393    .2697    right     7.516   13.369
                                GnRt     GnRtdBic   GnLf     GnLfdBic
                                11.799   10.718     1.570    1.959
```

A spreadsheet or other program can be set-up to handle as many entries as we might need to encompass a full pattern for the range of angles that we choose.

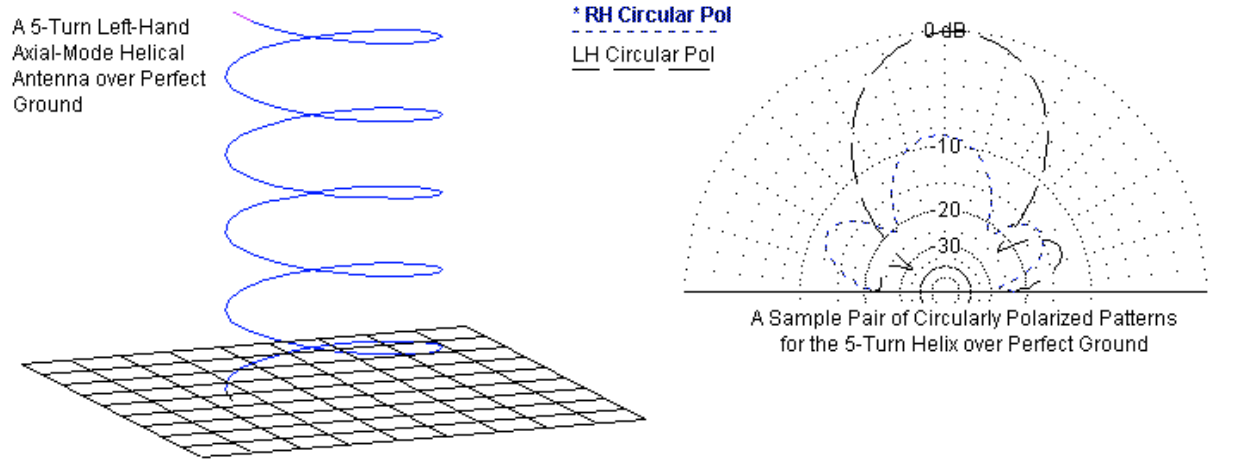

Fig. A2-2

As one final exercise, let's see what happens for a helix that is left-handed, as in the following example. See **Fig. A2-2**. Very little has changed, but the changes make a world of difference. Only the tilt angle and the Etheta phase angle have different numbers. However, those numbers alter the circular polarization calculations.

```
Theta      ERM      ELM      Sense    RatSq    PwrGn
0          .2697    .7393    left      0.133   13.369
                                GnRt     GnRtdBic   GnLf     GnLfdBic
                                1.570    1.959      11.799   10.718

Reference:  Corresponding line for the right-hand helix
0          .7393    .2697    right     7.516   13.369
                                11.799   10.718     1.570    1.959
```

The values for the zenith angle show a flip-flop that is not true of the values for the entire pair of left- and right-hand patterns. The right portion of **Fig. A-2** shows some of the detail. Below the zenith angle, the patterns for the left- and right-handed versions of the helix differ considerably--at least when examining them for fine detail. A comparison of the two model views in **Fig. A-1**and **Fig. A-2** will uncover the basic reason. The left-hand helix uses the same phi angle as the right-hand helix, but departs the ground plane at essentially a 90° angular difference to produce a true mirror image of the right-hand helix patterns. The left-hand patterns are a mirror image of the patterns we might obtain for the other helix by giving it a 90° phi-angle adjustment.

This exercise has provided a procedure by which you can calculate your own circular power gain patterns, if you are using an implementation of NEC that does not include them. Since they involve only data within the RP 0 section of the output report, the calculations are equally applicable to NEC-2 and NEC-4, even though the sample model is from NEC-4. If you already have provision for obtaining circularly polarized power gain patterns in your implementation of NEC, then perhaps the exercise will provide some insight into at least one way to obtain them.